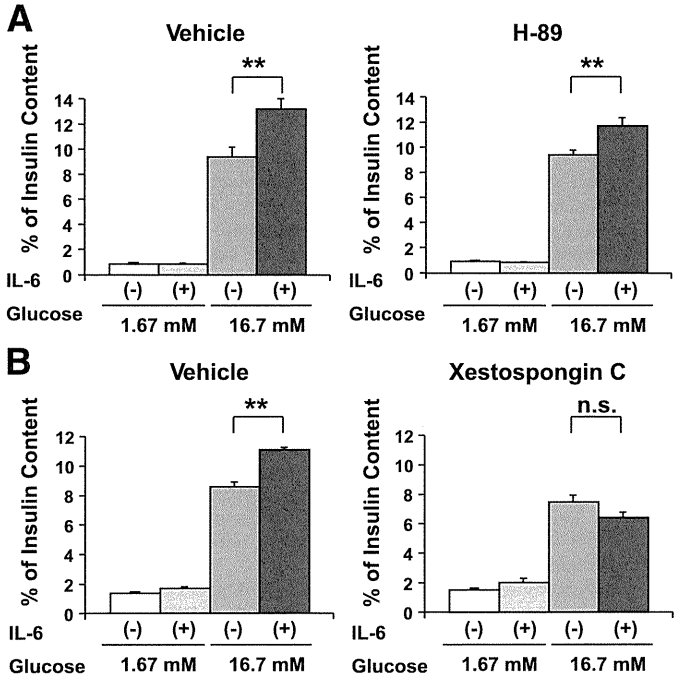

FIG. 6. IL-6–induced enhancement of GSIS is abrogated by an IP_3 receptor antagonist but not by a PKA inhibitor. MIN-6 cells were pretreated with vehicle or a pharmacological inhibitor (1 μmol/L H-89 [*A*] or 10 μmol/L Xestospongin C [*B*]) with or without concomitant 1,200 pg/mL IL-6 for 24 h, followed by measurement of insulin secretion for 60 min in KRBB supplemented with either 1.67 or 16.7 mmol/L glucose (n = 6 per group). **P < 0.01 vs. insulin secretion from MIN-6 cells without IL-6 pretreatment assessed by one-way ANOVA followed by Bonferroni's post hoc test. Data are presented as means ± SE.

consistent effects of IL-6 on insulin secretion have not been reported. At 1,500 pg/mL, IL-6 increased basal insulin secretion from murine isolated islets (4), and at 100 pg/mL, IL-6 increased both basal and glucose-stimulated insulin secretion from HIT-15 cells, a hamster β-cell line (5). On the other hand, 500–2,000 pg/mL (6) or 200–2,000 pg/mL (7) of IL-6 decreased GSIS from rat isolated pancreatic islets and 400 pg/mL IL-6 decreased GSIS from mouse isolated pancreatic islets (8). Furthermore, 400,000 pg/mL IL-6 did not alter insulin secretion from MIN-6 cells (9). Although the reason is unclear, these inconsistencies might be due to the different IL-6 concentrations and preincubation periods as well as sources of pancreatic β-cells used in the experiments. Therefore, in the current study, to elucidate the role of obesity-induced hyper-IL-6-emia in insulin secretion, we focused on IL-6 concentrations within the range of those observed in *ob/ob* and *db/db* mice, 150–7,000 pg/mL (20–22) in both in vivo and in vitro experiments. In addition, a circulating IL-6 level as high as 3,400 pg/mL was reported in obese human subjects (41). In the present in vivo study, plasma IL-6 concentrations were elevated and remained at 900–1,400 pg/mL during first the 10 days after adenoviral IL-6 expression in the liver. We used a similar concentration, 1,200 pg/mL, of IL-6 in our in vitro experiments.

We analyzed IL-6 effects on insulin secretion comparing three different settings of pancreatic β-cells, i.e., murine in vivo, isolated pancreatic islets ex vivo, and a pancreatic β-cell line, MIN-6 cells in vitro. Notably, all experiments showed IL-6–induced enhancement of GSIS, suggesting a direct effect of IL-6 on pancreatic β-cells. In addition, IL-6R knockdown, PLC inhibitors, and an IP_3 receptor antagonist almost completely inhibited the IL-6–induced enhancement of GSIS. PLC activation reportedly leads to hydrolysis of PIP_2 into diacylglycerol and IP_3. IP_3 binds to the IP_3 receptor on the ER, resulting in the induction of Ca^{2+} release from the ER. This raises the cytoplasmic free Ca^{2+} concentration and subsequently enhances insulin secretion (39). Our findings indicate that activation of the PLC-IP_3–dependent pathway by IL-6 appears to play a major role in GSIS enhancement during hyper-IL-6-emia. Activation of the PLC pathway by IL-6 signaling has been reported in several cell types. For instance, direct association of gp130 and PLC-γ was shown in a Ewing's sarcoma cell line (33). Activation of PLC-γ_1 by IL-6 was also reported in a pheochromocytoma cell line (34). On the other hand, in this study, siRNA experiments revealed knockdown of PLC-β_1, but not other isoforms, significantly to blunt IL-6–induced GSIS. Because the degrees of expression suppression differed among siRNAs specific for each PLC isoform (Supplementary Fig. 1), these results do not exclude the possibility that other PLC isoforms contribute to IL-6-induced GSIS. However, the data strongly suggest involvement of PLC-β_1 itself in the underlying mechanism. PLC-β_1 is reportedly activated by G protein-coupled receptors (42). Taken together with the results that long incubation periods, i.e., 24 h, were required for the stimulatory effects of IL-6 on GSIS, unknown mechanisms involving transcriptional or posttranscriptional alterations in certain molecules might mediate between the IL-6R and G protein-coupled receptor pathways.

Stimulatory effects of IL-6 on GSIS were also suggested in IL-6-KO mice (3). In HF-fed IL-6-KO mice, GSIS was impaired without alterations in pancreatic β-cell mass, resulting in postprandial hyperglycemia. The authors mainly analyzed the effects of IL-6 on pancreatic α-cell expansion, since IL-6-KO mice exhibited low glucagon levels with impaired pancreatic α-cell expansion (3). In the current study, plasma glucagon concentrations were significantly higher in IL-6 mice. In addition, interestingly, IL-6 enhanced GSIS more robustly in vivo and in isolated islets than that in MIN-6 cells (compare Fig. 3*B* and 4*A* with 4*B*). These findings suggest that the effects of IL-6 on glucagon secretion from pancreatic α-cells may have some impact on insulin secretion from β-cells in both in vivo and ex vivo experiments, in addition to the direct effects of IL-6 on β-cells.

Is the observed IL-6–mediated enhancement of GSIS involved in physiological or pathological states? Obesity leads to elevation of circulating IL-6. Circulating IL-6 is reportedly related to fat mass, and this relationship is also observed in mildly obese human subjects (43), suggesting that circulating IL-6 increases in the early phase of obesity. Notably, in human subjects, early in the development of obesity, GSIS is enhanced (44), and insulin hypersecretion occurs before blood glucose elevation (45–47). In mice, IL-6 deficiency reportedly raises postprandial blood glucose levels after HF diet loading (48) mainly due to impaired GSIS (3). In addition, in human subjects, circulating IL-6 concentrations correlate positively with first-phase insulin secretion, and this correlation is independent of insulin resistance (11). Taken together, these observations suggest that the mechanism elucidated in this study might be involved in GSIS enhancement in the early stage of obesity development. We recently identified a neuronal pathway from the liver as being involved in hyperinsulinemia in obese mice (17). In this regard, insulin hypersecretion during obesity development appears to be mediated by both neuronal and humoral signals, which are thought to cooperatively regulate

systemic metabolism (49). These mechanisms likely contribute to maintaining glucose homeostasis during obesity development. Interestingly, during septic shock states, hypoglycemia is commonly observed and this phenomenon is explained by hyperinsulinemia (50,51). It is well-known that IL-6 is markedly elevated during septic shock. Collectively, our findings suggest that hyper-IL-6-emia is involved in the development of hyperinsulinemia in states of both obesity and septic shock.

In conclusion, in vivo, ex vivo, and in vitro experiments consistently demonstrated that IL-6 enhances GSIS from pancreatic β-cells and that this enhancement of GSIS is likely to be mediated by the PLC-IP_3–dependent pathway. Modulating the PLC pathway in pancreatic β-cells is a potential therapeutic strategy for achieving efficient postprandial insulin secretion.

ACKNOWLEDGMENTS

This work was supported by Grants-in-Aid for Scientific Research to H.K. (B2, 15390282) and Y.O. (A2, 19209034) from the Ministry of Education, Science, Sports and Culture of Japan and a Grant-in-Aid for Scientific Research (H19-genome-005) to Y.O. from the Ministry of Health, Labor and Welfare of Japan. This work was also supported by the Global-COE Program for Network Medicine to Y.O. and H.K. from the Ministry of Education, Culture, Sports, Science and Technology of Japan.

No potential conflicts of interest relevant to this article were reported.

T.S. and J.I. researched data, wrote the article, and contributed to discussion. T.Y., Y.I., K.K., K.U., Y.H., and H.I. contributed to discussion. Y.O. contributed to discussion and reviewed and edited the article. H.K. contributed to discussion and wrote the article.

The authors thank I. Sato, J. Fushimi, M. Aizawa, M. Hoshi, and T. Takasugi (Department of Metabolic Diseases, Center for Metabolic Diseases, Tohoku University Graduate School of Medicine) for technical support.

REFERENCES

1. Kristiansen OP, Mandrup-Poulsen T. Interleukin-6 and diabetes: the good, the bad, or the indifferent? Diabetes 2005;54(Suppl. 2):S114–S124
2. Hoene M, Weigert C. The role of interleukin-6 in insulin resistance, body fat distribution and energy balance. Obes Rev 2008;9:20–29
3. Ellingsgaard H, Ehses JA, Hammar EB, et al. Interleukin-6 regulates pancreatic alpha-cell mass expansion. Proc Natl Acad Sci USA 2008;105:13163–13168
4. Buschard K, Aaen K, Horn T, Van Damme J, Bendtzen K. Interleukin 6: a functional and structural in vitro modulator of beta-cells from islets of Langerhans. Autoimmunity 1990;5:185–194
5. Shimizu H, Ohtani K, Kato Y, Mori M. Interleukin-6 increases insulin secretion and preproinsulin mRNA expression via Ca^{2+}-dependent mechanism. J Endocrinol 2000;166:121–126
6. Sandler S, Bendtzen K, Eizirik DL, Welsh M. Interleukin-6 affects insulin secretion and glucose metabolism of rat pancreatic islets in vitro. Endocrinology 1990;126:1288–1294
7. Southern C, Schulster D, Green IC. Inhibition of insulin secretion from rat islets of Langerhans by interleukin-6. An effect distinct from that of interleukin-1. Biochem J 1990;272:243–245
8. Handschin C, Choi CS, Chin S, et al. Abnormal glucose homeostasis in skeletal muscle-specific PGC-1alpha knockout mice reveals skeletal muscle-pancreatic beta cell crosstalk. J Clin Invest 2007;117:3463–3474
9. Choi SE, Choi KM, Yoon IH, et al. IL-6 protects pancreatic islet beta cells from pro-inflammatory cytokines-induced cell death and functional impairment in vitro and in vivo. Transpl Immunol 2004;13:43–53
10. Franckhauser S, Elias I, Rotter Sopasakis V, et al. Overexpression of Il6 leads to hyperinsulinaemia, liver inflammation and reduced body weight in mice. Diabetologia 2008;51:1306–1316
11. Andreozzi F, Laratta E, Cardellini M, et al. Plasma interleukin-6 levels are independently associated with insulin secretion in a cohort of Italian-Caucasian nondiabetic subjects. Diabetes 2006;55:2021–2024
12. Imai J, Katagiri H, Yamada T, et al. Constitutively active PDX1 induced efficient insulin production in adult murine liver. Biochem Biophys Res Commun 2005;326:402–409
13. Yamada T, Katagiri H, Ishigaki Y, et al. Signals from intra-abdominal fat modulate insulin and leptin sensitivity through different mechanisms: neuronal involvement in food-intake regulation. Cell Metab 2006;3:223–229
14. Uno K, Katagiri H, Yamada T, et al. Neuronal pathway from the liver modulates energy expenditure and systemic insulin sensitivity. Science 2006;312:1656–1659
15. Katagiri H, Asano T, Ishihara H, et al. Overexpression of catalytic subunit p110alpha of phosphatidylinositol 3-kinase increases glucose transport activity with translocation of glucose transporters in 3T3-L1 adipocytes. J Biol Chem 1996;271:16987–16990
16. Ishihara H, Takeda S, Tamura A, et al. Disruption of the WFS1 gene in mice causes progressive beta-cell loss and impaired stimulus-secretion coupling in insulin secretion. Hum Mol Genet 2004;13:1159–1170
17. Imai J, Katagiri H, Yamada T, et al. Regulation of pancreatic beta cell mass by neuronal signals from the liver. Science 2008;322:1250–1254
18. Imai J, Katagiri H, Yamada T, et al. Cold exposure suppresses serum adiponectin levels through sympathetic nerve activation in mice. Obesity (Silver Spring) 2006;14:1132–1141
19. Ishigaki Y, Katagiri H, Yamada T, et al. Dissipating excess energy stored in the liver is a potential treatment strategy for diabetes associated with obesity. Diabetes 2005;54:322–332
20. Harkins JM, Moustaid-Moussa N, Chung YJ, et al. Expression of interleukin-6 is greater in preadipocytes than in adipocytes of 3T3-L1 cells and C57BL/6J and ob/ob mice. J Nutr 2004;134:2673–2677
21. Brun P, Castagliuolo I, Di Leo V, et al. Increased intestinal permeability in obese mice: new evidence in the pathogenesis of nonalcoholic steatohepatitis. Am J Physiol Gastrointest Liver Physiol 2007;292:G518–G525
22. Li M, Kim DH, Tsenovoy PL, et al. Treatment of obese diabetic mice with a heme oxygenase inducer reduces visceral and subcutaneous adiposity, increases adiponectin levels, and improves insulin sensitivity and glucose tolerance. Diabetes 2008;57:1526–1535
23. Wallenius V, Wallenius K, Ahrén B, et al. Interleukin-6-deficient mice develop mature-onset obesity. Nat Med 2002;8:75–79
24. Ropelle ER, Fernandes MF, Flores MB, et al. Central exercise action increases the AMPK and mTOR response to leptin. PLoS ONE 2008;3:e3856
25. Banks WA, Kastin AJ, Broadwell RD. Passage of cytokines across the blood-brain barrier. Neuroimmunomodulation 1995;2:241–248
26. Fasshauer M, Kralisch S, Klier M, et al. Adiponectin gene expression and secretion is inhibited by interleukin-6 in 3T3-L1 adipocytes. Biochem Biophys Res Commun 2003;301:1045–1050
27. Gustafson B, Smith U. Cytokines promote Wnt signaling and inflammation and impair the normal differentiation and lipid accumulation in 3T3-L1 preadipocytes. J Biol Chem 2006;281:9507–9516
28. Inoue H, Ogawa W, Ozaki M, et al. Role of STAT-3 in regulation of hepatic gluconeogenic genes and carbohydrate metabolism in vivo. Nat Med 2004;10:168–174
29. Petersen EW, Carey AL, Sacchetti M, et al. Acute IL-6 treatment increases fatty acid turnover in elderly humans in vivo and in tissue culture in vitro. Am J Physiol Endocrinol Metab 2005;288:E155–E162
30. Itoh Y, Kawamata Y, Harada M, et al. Free fatty acids regulate insulin secretion from pancreatic beta cells through GPR40. Nature 2003;422:173–176
31. Ishihara H, Asano T, Tsukuda K, et al. Pancreatic beta cell line MIN6 exhibits characteristics of glucose metabolism and glucose-stimulated insulin secretion similar to those of normal islets. Diabetologia 1993;36:1139–1145
32. Gilon P, Henquin JC. Mechanisms and physiological significance of the cholinergic control of pancreatic beta-cell function. Endocr Rev 2001;22:565–604
33. Boulton TG, Stahl N, Yancopoulos GD. Ciliary neurotrophic factor/leukemia inhibitory factor/interleukin 6/oncostatin M family of cytokines induces tyrosine phosphorylation of a common set of proteins overlapping those induced by other cytokines and growth factors. J Biol Chem 1994;269:11648–11655
34. Lee YH, Bae SS, Seo JK, Choi I, Ryu SH, Suh PG. Interleukin-6-induced tyrosine phosphorylation of phospholipase C-gamma1 in PC12 cells. Mol Cells 2000;10:469–474
35. Fujiwara K, Maekawa F, Yada T. Oleic acid interacts with GPR40 to induce Ca^{2+} signaling in rat islet beta-cells: mediation by PLC and L-type Ca^{2+} channel and link to insulin release. Am J Physiol Endocrinol Metab 2005;289:E670–E677

36. Kelley GG, Zawalich KC, Zawalich WS. Synergistic interaction of glucose and neurohumoral agonists to stimulate islet phosphoinositide hydrolysis. Am J Physiol 1995;269:E575–E582
37. Gasa R, Trinh KY, Yu K, Wilkie TM, Newgard CB. Overexpression of G11alpha and isoforms of phospholipase C in islet beta-cells reveals a lack of correlation between inositol phosphate accumulation and insulin secretion. Diabetes 1999;48:1035–1044
38. Light PE, Manning Fox JE, Riedel MJ, Wheeler MB. Glucagon-like peptide-1 inhibits pancreatic ATP-sensitive potassium channels via a protein kinase A- and ADP-dependent mechanism. Mol Endocrinol 2002;16:2135–2144
39. Ahrén B. Islet G protein-coupled receptors as potential targets for treatment of type 2 diabetes. Nat Rev Drug Discov 2009;8:369–385
40. Tsuboi T, da Silva Xavier G, Holz GG, Jouaville LS, Thomas AP, Rutter GA. Glucagon-like peptide-1 mobilizes intracellular Ca^{2+} and stimulates mitochondrial ATP synthesis in pancreatic MIN6 beta-cells. Biochem J 2003;369: 287–299
41. Teramoto S, Yamamoto H, Ouchi Y. Increased plasma interleukin-6 is associated with the pathogenesis of obstructive sleep apnea syndrome. Chest 2004;125:1964–1965
42. Rebecchi MJ, Pentyala SN. Structure, function, and control of phosphoinositide-specific phospholipase C. Physiol Rev 2000;80:1291–1335
43. Carey AL, Bruce CR, Sacchetti M, et al. Interleukin-6 and tumor necrosis factor-alpha are not increased in patients with type 2 diabetes: evidence that plasma interleukin-6 is related to fat mass and not insulin responsiveness. Diabetologia 2004;47:1029–1037
44. Le Stunff C, Bougnères P. Early changes in postprandial insulin secretion, not in insulin sensitivity, characterize juvenile obesity. Diabetes 1994;43:696–702
45. Dubuc PU. The development of obesity, hyperinsulinemia, and hyperglycemia in ob/ob mice. Metabolism 1976;25:1567–1574
46. Blonz ER, Stern JS, Curry DL. Dynamics of pancreatic insulin release in young Zucker rats: a heterozygote effect. Am J Physiol 1985;248:E188–E193
47. Utzschneider KM, Prigeon RL, Carr DB, et al. Impact of differences in fasting glucose and glucose tolerance on the hyperbolic relationship between insulin sensitivity and insulin responses. Diabetes Care 2006;29: 356–362
48. Di Gregorio GB, Hensley L, Lu T, Ranganathan G, Kern PA. Lipid and carbohydrate metabolism in mice with a targeted mutation in the IL-6 gene: absence of development of age-related obesity. Am J Physiol Endocrinol Metab 2004;287:E182–E187
49. Katagiri H, Yamada T, Oka Y. Adiposity and cardiovascular disorders: disturbance of the regulatory system consisting of humoral and neuronal signals. Circ Res 2007;101:27–39
50. Filkins JP. Phases of glucose dyshomeostasis in endotoxicosis. Circ Shock 1978;5:347–355
51. Yelich MR. Effects of naloxone on glucose and insulin regulation during endotoxicosis in fed and fasted rats. Circ Shock 1988;26:273–285

THE JOURNAL OF BIOLOGICAL CHEMISTRY VOL. 285, NO. 43, pp. 33018–33027, October 22, 2010

Pin1 Associates with and Induces Translocation of CRTC2 to the Cytosol, Thereby Suppressing cAMP-responsive Element Transcriptional Activity*[S]

Received for publication, April 26, 2010, and in revised form, July 9, 2010 Published, JBC Papers in Press, July 30, 2010, DOI 10.1074/jbc.M110.137836

Yusuke Nakatsu,[a1] Hideyuki Sakoda,[b1] Akifumi Kushiyama,[c] Hiraku Ono,[b] Midori Fujishiro,[b] Nanao Horike,[d] Masayasu Yoneda,[a] Haruya Ohno,[a] Yoshihiro Tsuchiya,[a] Hideaki Kamata,[a] Hidetoshi Tahara,[e] Toshiaki Isobe,[f] Fusanori Nishimura,[g] Hideki Katagiri,[h] Yoshitomo Oka,[h] Toshiaki Fukushima,[a] Shin-Ichiro Takahashi,[i] Hiroki Kurihara,[d] Takafumi Uchida,[j] and Tomoichiro Asano[a2]

From the [a]Department of Medical Science, Graduate School of Medicine, University of Hiroshima, 1-2-3 Kasumi, Minami-ku, Hiroshima City, Hiroshima 734-8553, Japan, the Departments of [b]Internal Medicine and [d]Physiological Chemistry and Metabolism, Graduate School of Medicine, and the [i]Department of Applied Biological Chemistry, Graduate School of Agricultural and Life Sciences, University of Tokyo, 7-3-1 Hongo, Bunkyo-ku, Tokyo 113-0033, Japan, the [c]Institute for Adult Disease, Asahi Life Foundation, Tokyo 100-0006, Japan, the [e]Department of Cellular and Molecular Biology, Graduate School of Biomedical Sciences, Hiroshima University, Hiroshima 734-8553, Japan, the [f]Center for Priority Areas, Tokyo Metropolitan University, Hachioji, Tokyo 192-0397, Japan, the [g]Department of Dental Science for Health Promotion, Hiroshima University Graduate School of Biomedical Sciences, Hiroshima 734-8553, Japan, the [h]Division of Molecular Metabolism and Diabetes, Tohoku University Graduate School of Medicine, 2-1 Seiryo-machi, Aoba-ku, Sendai 980-8575, Japan, and the [j]Department of Molecular Cell Biology, Graduate School of Agricultural Science, Tohoku University, Sendai, Miyagi 981-8555, Japan

Pin1 is a unique regulator, which catalyzes the conversion of a specific phospho-Ser/Thr-Pro-containing motif in target proteins. Herein, we identified CRTC2 as a Pin1-binding protein by overexpressing Pin1 with Myc and FLAG tags in mouse livers and subsequent purification of the complex containing Pin1. The association between Pin1 and CRTC2 was observed not only in overexpression experiments but also endogenously in the mouse liver. Interestingly, Ser^{136} in the nuclear localization signal of CRTC2 was shown to be involved in the association with Pin1. Pin1 overexpression in HepG2 cells attenuated forskolin-induced nuclear localization of CRTC2 and cAMP-responsive element (CRE) transcriptional activity, whereas gene knockdown of Pin1 by siRNA enhanced both. Pin1 also associated with CRTC1, leading to their cytosol localization, essentially similar to the action of CRTC2. Furthermore, it was shown that CRTC2 associated with Pin1 did not bind to CREB. Taken together, these observations indicate the association of Pin1 with CRTC2 to decrease the nuclear CBP·CRTC·CREB complex. Indeed, adenoviral gene transfer of Pin1 into diabetic mice improved hyperglycemia in conjunction with normalizing phosphoenolpyruvate carboxykinase mRNA expression levels, which is regulated by CRE transcriptional activity. In conclusion, Pin1 regulates CRE transcriptional activity, by associating with CRTC1 or CRTC2.

Pin1 was initially cloned as a NIMA kinase-interacting protein (1). Since its discovery, numerous proteins have been identified as Pin1 substrates, including p53, cyclin D1, and Tau (2–5). Pin1 interacts with a number of target proteins through recognition of phospho-Ser/Pro motifs, and the proline conformational change induced by Pin1 modifies the structures and functions, such as stabilization, phosphorylation, and translocation, of target proteins (4–7). Pin1 possesses the WW and PPIase[3] domains in its N-terminal (amino acids 1–38) and C-terminal (amino acids 39–163) regions, respectively. To date, many reports have supported an important role for Pin1 in diseases such as cancer and Alzheimer disease (4, 5). In this study, we demonstrated that Pin1 is also involved in metabolic disease via regulation of CRTC2 (CREB-regulated transcriptional co-activator 2; also known as TORC).

The cAMP-responsive element (CRE)-binding protein (CREB) stimulates transcriptional activity through recruitment of the histone acetylase CBP and through an association with CRTC, leading to formation of the CREB·CBP·CTRC complex on a CRE site (8–16). Thus, multiple molecular mechanisms affect the CREB·CBP·CTRC complex, resulting in the regulation of CRE transcriptional activity. They include the phosphorylations of CREB at Ser^{133}, CBP at Ser^{436}, and CRTC2 at Ser^{171} (16, 17). The phosphorylation of CRTC2 at Ser^{171} reportedly leads to an association with 14-3-3 protein and thereby to its nuclear exclusion and degradation (16).

The CRTC family consists of three members, CRTC1, CRTC2, and CRTC3 (16, 18). CRTC1 is highly expressed in the brain, whereas the other two are ubiquitously expressed (19). In the liver, insulin induces the phosphorylation of CRTC2 at Ser^{171}, and this phosphorylation leads to the aforementioned

* This work was supported in part by Grant-in-aid for Young Scientists 20790648 (to Y. N.) from the Ministry of Education, Science, Sports, and Culture, Japan.

[S] The on-line version of this article (available at http://www.jbc.org) contains supplemental Figs. 1–8.

[1] These authors contributed equally to this work.

[2] To whom correspondence should be addressed. Tel.: 81-82-257-5135; Fax: 81-82-257-5136; E-mail: asano-tky@umin.ac.jp.

[3] The abbreviations used are: PPIase, peptidyl-prolyl *cis/trans*-isomerase; CRE, cAMP-response element; CREB, CRE-binding protein; NLS, nuclear localization signal; MEF, mouse embryo fibroblast; STZ, streptozotocin; PEPCK, phosphoenolpyruvate carboxykinase; CRTC, CREB-regulated transcriptional co-activator.

association with 14-3-3 protein and the nuclear exclusion and degradation of CRTC2 (16, 20). In contrast, glucagon induces dephosphorylation of CRTC2 and translocation from the cytosol to the nucleus, thereby forming the CREB·CBP·CRTC2 complex and inducing gluconeogenesis (21). Thus, CRTC2 plays important roles in hepatic glucose metabolism.

In this study, we identified CRTC2 as a Pin1-binding protein. Interestingly, the portion of CRTC2 responsible for the association with Pin1 was revealed to be in the nuclear localization signal (NLS) domain. Herein, we demonstrate that Pin1 regulates the functions and subcellular localizations of CRTC family proteins, thereby altering CRE transcriptional activity.

EXPERIMENTAL PROCEDURES

Materials—Anti-Pin1 antibody was generated by immunizing rabbits with the peptide QMQKPFEDASFATRTGEMSGPVFTDSGIHIITRTE (amino acids 129–163 of human Pin1). Anti-FLAG tag and Myc tag antibodies were purchased from Sigma-Aldrich. The antibodies against CRTC2, CREB, 14-3-3 protein, GFP, and DsRed were purchased from Cell Signaling Technology. Anti-rabbit HRP antibodies conjugated to horseradish peroxidase were obtained from Amersham Biosciences. Dulbecco's modified Eagle's medium (DMEM) and fetal bovine serum were purchased from Invitrogen. All other reagents were of analytical grade.

Preparation of Adenoviruses Expressing MEF-tagged Pin1, CRTC1, and CRTC2—The Myc-TEV-FLAG (MEF) tag cassette was generated by DNA synthesis and inserted into cloning sites in the mammalian expression vector pcDNA3 (Invitrogen; termed pcDNA3-MEF), as reported previously (22). To create the N-terminally MEF-tagged Pin1 construct, human Pin1 cDNA was inserted into pcDNA3-MEF. Then the coding portion of MEF-tagged Pin1 was isolated from pcDNA3-MEF-Pin1, and the recombinant adenoviruses containing the cDNA coding for MEF-tagged Pin1 were constructed as described previously (22). Recombinant adenoviruses expressing human Pin1 with the C-terminal HA tag or N-terminal MEF tag were also constructed and used for adenoviral gene transfer to HepG2 cells and mouse liver. Similarly, adenoviruses expressing GFP-tagged CTRC1, CRTC2, and GFP-tagged CRTC2 were prepared. Adenovirus encoding LacZ served as a control, and the adenoviral gene transfer was performed as reported previously (22).

Purification of MEF-tagged Pin1 from Mouse Livers—Recombinant adenovirus expressing MEF-tagged Pin1 was generated, purified, and concentrated using cesium chloride ultracentrifugation as reported previously (22). Adenovirus encoding LacZ served as a control. Male mice, 9 weeks of age, were obtained from the Nippon Bio-Supp. Center (Tokyo, Japan). They were injected, via the tail vein, with adenovirus at a dose of 2.5×10^7 plaque-forming units/g body weight. Four days after adenovirus injection, the mouse livers were removed and lysed in lysis buffer (50 mM Tris-HCl, pH 7.5, 150 mM NaCl, 10% (w/v) glycerol, 100 mM NaF, 10 mM EGTA, 1 mM Na_3VO_4, 1% (w/v) Triton X-100, 5 μM $ZnCl_2$, 2 mM phenylmethylsulfonyl fluoride, 10 μg/ml aprotinin, and 1 μg/ml leupeptin). The lysates were centrifuged at 100,000 × *g* for 20 min at 4 °C. The supernatant was passed through a 5-μm filter, incubated with 150 μl of Sepharose beads for 60 min at 4 °C and then passed through a 0.65-μm filter. The filtrated supernatant was mixed with 150 μl of anti-Myc-conjugated Sepharose beads for the first immunoprecipitation. After incubation for 90 min at 4 °C, the beads were washed five times with 1.5 ml of TNTG buffer (20 mM Tris-HCl, pH 7.5, 150 mM NaCl, 10% (w/v) glycerol, 0.1% (w/v) Triton X-100), twice with buffer A (20 mM Tris-HCl, pH 7.5, 150 mM NaCl, and 0.1% (w/v) Triton X-100), and finally once with TNT buffer (50 mM Tris-HCl, pH 8.0, 150 mM NaCl, 0.1% (w/v) Triton X-100). The washed beads were incubated with 15 units of TEV protease (Invitrogen) in 150 μl of TNT buffer to release bound materials from the beads. After incubation for 60 min at room temperature, the supernatant was pooled, and the beads were washed twice with 75 μl of buffer A. The resulting supernatants were combined and incubated with 25 μl of FLAG-Sepharose beads for the second immunoprecipitation. After incubation for 60 min at room temperature, the beads were washed three times with 500 μl of buffer A, and proteins bound to the FLAG beads were dissociated by incubation with 1 mM synthetic FLAG peptides in buffer A for 120 min at 4 °C. Approximately 3 μg of protein (0.01% of starting materials) were routinely recovered by this procedure. The samples were electrophoresed and subjected to SDS-PAGE and immunoblotting.

Cell Culture—Sf9 cells were grown in TC100 (Invitrogen) medium containing 10% fetal calf serum at 27 °C. HepG2 hepatoma cells were grown in DMEM containing 10% fetal calf serum at 37 °C in 5% (v/v) CO_2 in air.

Preparation of Baculoviruses Expressing Pin1 and CRTC2 Constructs—The full-length coding regions of human Pin1, GFP, GFP-tagged Pin1, CRTC2, and DsRed-tagged full-length and various deletion mutant forms of CRTC2 and S136A CRTC2 were subcloned into pBacPAK9 transfer vector (Clontech), and the baculoviruses were prepared according to the manufacturer's instructions. For protein production, Sf9 cells were infected with these baculoviruses and grown for 48 h.

Preparation of Glutathione S-Transferase (GST)-Pin1 Fusion Protein—The cDNAs encoding full-length human Pin1, the WW domain of Pin1, and the PPIase domain of Pin1 were subcloned into a pGEX-5X-1 vector (Amersham Biosciences), which was used to transform *Escherichia coli* JM105 (Promega). Transformed cells were grown to an A_{600} of 0.6 in LB medium supplemented with 0.1 mg/ml ampicillin and stimulated for 3 h with 1.0 mM isopropyl-β-D-thiogalactopyranoside. GST fusion proteins were conjugated to glutathione-Sepharose 4B (Amersham Biosciences) and used for GST pull-down experiments.

GST Pull-down—HepG2 cells expressing MEF-CTRC2 and its mutants were homogenized with homogenizing buffer (20 mmol/liter Tris/HCl (pH 7.4), 1% Triton X-100, 0.25% sodium deoxycholate, 0.25 mol/liter NaCl) containing 0.2 mmol/liter phenylmethylsulfonyl fluoride and 5 μg/ml aprotinin and centrifuged at 15,000 rpm for 30 min at 4 °C, and the supernatants were then recentrifuged at 100,000 × *g* for 1 h. The supernatants (2 μg/ml protein concentration) were incubated with 1 ml of glutathione-Sepharose 4B for 1 h at 4 °C to remove nonspecifically bound proteins and then incubated with purified GST alone, GST-Pin1, and GST-Pin1 deletion mutant proteins for 1 h and finally washed six times with homogenizing buffer. glutathione-Sepharose 4B beads

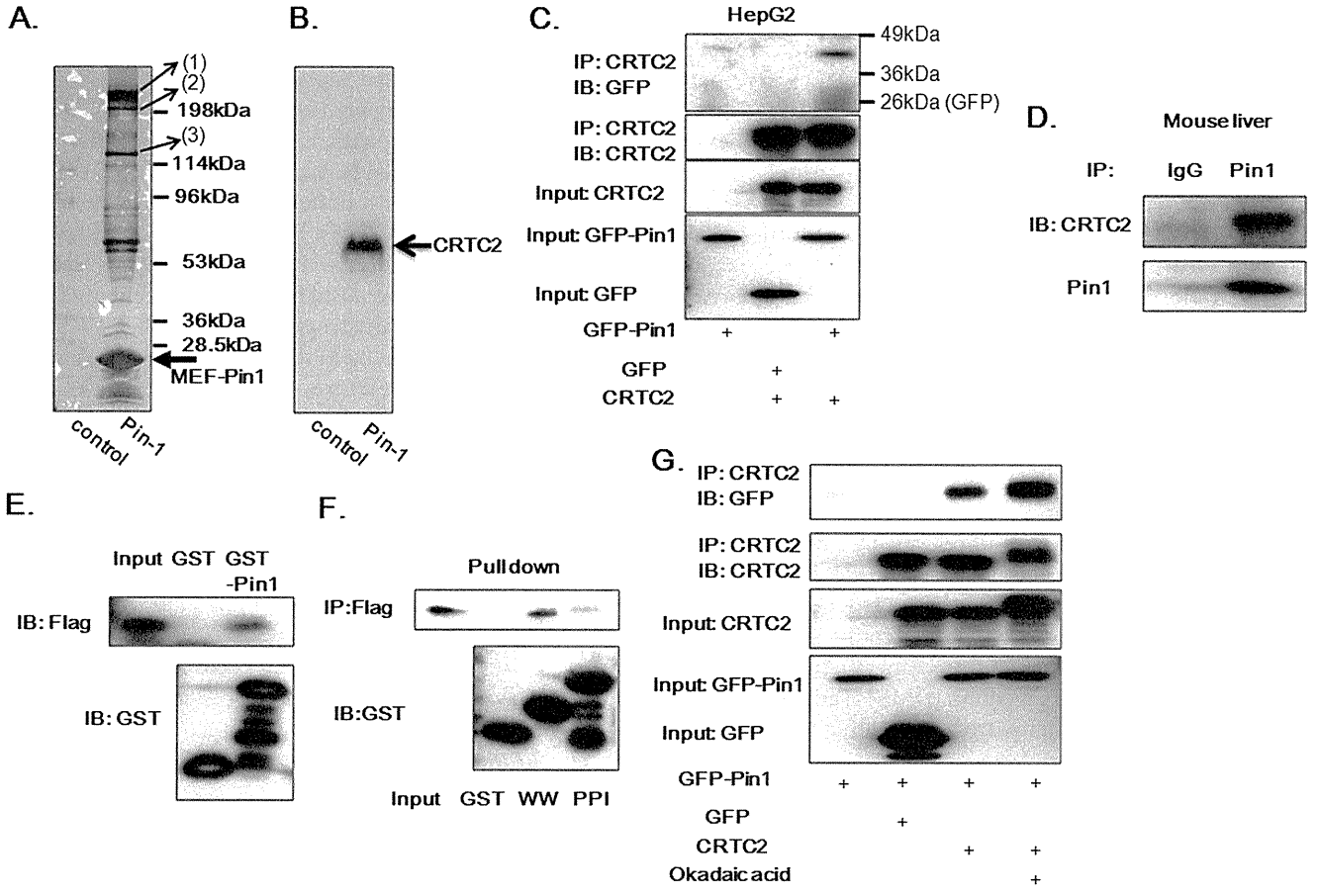

FIGURE 1. **Pin1 associates with CRTC2.** *A* and *B*, Pin1 with the N-terminal MEF tag was overexpressed in the mouse liver using adenovirus gene transfer, and the Pin1-containing complex was purified. The samples were electrophoresed and subjected to silver staining (*A*). Analysis using LC/MS revealed: *Band* (*1*), DNA-directed RNA polymerase II A; *Band* (*2*), suppressor of Ty 6 homolog + DNA-directed RNA polymerase II A; *Band* (*3*), DNA-directed RNA polymerase II polypeptide B + DNA-directed RNA polymerase I. *B*, the samples were subjected to the immunoblotting with anti-CRTC2 antibody. *C*, CRTC2 or control LacZ was overexpressed with GFP or GFP-Pin1. Then the cell lysates were immunoprecipitated (*IP*) with anti-CRTC2 antibody, followed by immunoblotting (*IB*) with anti-GFP antibody. *D*, the cell lysates from the mouse liver were immunoprecipitated with control IgG or anti-Pin1, and the immunoprecipitates were then immunoblotted with anti-CRTC2 and anti-Pin-1. *E*, HepG2 cell lysates expressing CRTC2 with a FLAG tag were incubated with glutathione beads conjugated with GST or GST-Pin1. After washing the beads, SDS-PAGE was performed followed by immunoblotting with anti-FLAG or anti-GST antibodies. *F*, HepG2 cell lysates expressing CRTC2 with a FLAG tag were incubated with glutathione beads conjugated with GST, the GST-WW domain, or the GST-PPI domain. After washing the beads, SDS-PAGE was performed, followed by immunoblotting with anti-FLAG or anti-GST antibodies. *G*, CRTC2 and either GFP or GFP-Pin1 were simultaneously overexpressed in HepG2 cells. With or without okadaic acid treatment for 0.5 h, the cell lysates were immunoprecipitated with anti-CRTC2, followed by immunoblotting with anti-GFP antibody. Representative immunoblotting data from three independent experiments are shown.

were boiled in Laemmli sample buffer, which was used for the SDS-PAGE and immunoblotting.

Preparation of Streptozotocin-treated Diabetic Mice and Gene Transfer of Pin1 into Mouse Livers—Streptozotocin (STZ)-treated diabetic male C57BL/6 mice (8–10 weeks of age) were prepared as reported previously (20). These mice were injected, via the tail vein, with adenovirus at a dose of 2.5×10^7 plaque-forming units/g body weight. Animals were fasted for 14 h and then were refed for 4 h before sacrifice. Blood glucose was measured with a portable blood glucose monitor, Glutest-Ace (Sanwa Kagaku Kenkyusho, Nagoya, Japan). All animal studies were conducted according to the Japanese guidelines for the care and use of experimental animals.

Immunoprecipitation and Immunoblotting—For the immunoprecipitation experiments, whole-cell extracts from HepG2 or Sf9 cells or mouse liver lysates obtained after an overnight fast were prepared in lysis buffer, as described above. Cell or tissue extracts were incubated for 4 h at 4 °C with the indicated antibody and then for 1 h with 30 μl of protein G-Sepharose beads. The pellets were washed five times with 1 ml of lysis buffer and then resuspended in Laemmli sample buffer, boiled for 3 min, and analyzed on SDS-polyacrylamide gels.

Western blot analysis was carried out as described previously (22). In brief, 10 μg of protein were separated by SDS-PAGE and electrophoretically transferred to polyvinylidene difluoride membranes in a transfer buffer consisting of 20 mM Tris-HCl, 150 mM glycine, and 20% methanol. The membranes were blocked with 5% nonfat dry milk in Tris-buffered saline with 0.1% Tween 20 and incubated with specific antibodies, followed by incubation with horseradish peroxidase-conjugated secondary antibodies. The antigen-antibody interactions were visualized by incubation with ECL chemiluminescence reagent (Amersham Biosciences).

Immunostaining—HepG2 cells were fixed with 4% paraformaldehyde for 10 min, rinsed with phosphate-buffered saline (PBS), and then exposed to 0.2% Triton X-100 in PBS for 5 min. Cells were subsequently incubated for 1 h at room temperature with anti-rabbit CRTC2 (1:500), and fluorescein isothiocya-

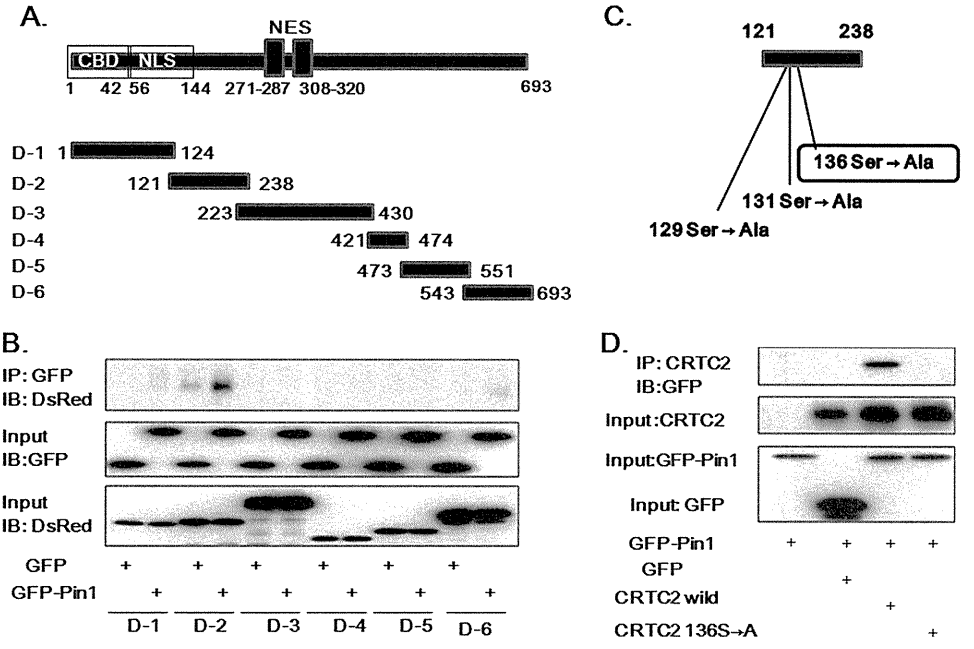

FIGURE 2. **Pin1 associates with the NLS domain of CRTC2.** *A*, the constructs of CRTC2 deletion mutants and baculoviruses expressing these six mutants with the C-terminal DsRed tag were prepared. *B*, the six deletion mutants with C-terminal DsRed tags were overexpressed with GFP or GFP-Pin1 in Sf9 cells. The cell lysates were immunoprecipitated (*IP*) with anti-GFP antibody, followed by immunoblotting (*IB*) with anti-DsRed antibody. The *upper panel* shows the binding of the Deletion-2 mutant to GFP-Pin1 but not to GFP alone. *C*, the orientations of three candidate Ser/Pro motifs in the Deletion-2 mutant involved in the association with Pin1. *D*, wild-type CRTC2 or CRTC2 S136A was overexpressed with GFP-Pin1 or GFP in Sf9 cells. The cell lysates were immunoprecipitated with anti-CRTC2 antibody followed by immunoblotting with anti-GFP. The *upper panel* shows that CRTC2 S136A does not associate with Pin1, unlike the wild-type CRTC2. Representative immunoblotting data from three independent experiments are shown.

nate-labeled anti-rabbit IgG (1:750) was used as the secondary antibody. Immunofluorescence was visualized with a laser-scanning confocal imaging system.

Luciferase Assay—The following plasmids were obtained from commercial sources: pTAL and pTAL-CRE from Clontech (Palo Alto, CA), pM from Stratagene (La Jolla, CA), and pGL4 and pRL-TK from Promega (Madison, WI). HepG2 cells in a 24-well collagen-coated plate were co-transfected with pTAL-CRE vector (0.25 μg/well) with an internal reporter, pRL-TK (0.25 μg). Luciferase activities were determined using the Dual-Luciferase Reporter Assay System (Promega Corp.).

RNA Analysis—RNA extractions were carried out using TRIzol, followed by purification over a QIAEASY RNA column. Reverse transcription and quantitative PCR were carried out as already described. The primer set for human phosphoenolpyruvate carboxykinase (PEPCK) was GGTTCCCAGGGTGCATGAAA and CACGTAGGGTGAATCCGTCAG (114 bp), and that for human GAPDH was ACCACAGTCCATGCCATCAC and TCCACCACCCTGTTGCTGTA (451 bp).

Chromatin Immunoprecipitation Assay with Anti-CRTC2, CBP, or CREB Antibodies—HepG2 cells with or without forskolin stimulation were immunoprecipitated with anti-CRTC2, anti-CBP, or anti-CREB antibody, using the Chip-IT™ express enzymatic kit (Active Motif Corp.). Then precipitated DNA was amplified by PCR using primers against the relevant promoters.

Statistical Analysis—Results are expressed as means ± S.E., and significance was assessed using one-way analysis of variance unless otherwise indicated.

RESULTS

Identification of CRTC2 in the Pin1-containing Complex from Mouse Liver—The adenovirus to MEF-tagged Pin1 was introduced into mice, and the Pin1-containing complex was purified. Purified Pin1 in the complex was electrophoresed and subjected to silver staining, which showed the presence of Pin1 bait proteins and many binding proteins (Fig. 1*A*). Bands (1), (2), and (3) were identified to be DNA-directed RNA polymerase II A, DNA-directed RNA polymerase IIB, and DNA-directed RNA polymerase I by the analysis using LC/MS, which agree with previous reports (23). Then we performed the immunoblotting using many antibodies to detect another protein included in the Pin1-containing complex because many faint bands were visible with silver staining.

Many transcriptional co-activators are included among the target proteins of Pin1 (4, 5). In addition, although one of the regulatory mechanisms of Pin1 is protein stabilization, recent reports have shown that Pin1 is involved in translocation of target proteins, such as Bax (24). These results suggest that CRTC2 is a candidate Pin1 target protein because CRTC2 is a transcriptional co-activator and is translocated between the cytosol and the nucleus. As a result, immunoblotting using anti-CRTC2 antibody indicated the presence of CTRC2 in the Pin1 complexes (Fig. 1*B*). To confirm the association between CTRC2 and Pin1, CRTC2 and each GFP-Pin1 or GFP were simultaneously overexpressed in HepG2 and Sf9 cells. As shown in Fig. 1*C* and supplemental Fig. 1, GFP-Pin1, but not GFP alone was detected in the anti-CRTC2 immunoprecipitate. Furthermore, CRTC2 was detected in the immunoprecipitate with anti-Pin1 antibody but not that with the control IgG from mouse liver (Fig. 1*D*). Thus, the association between CRTC2 and Pin1 is physiological.

Pin1 possesses the WW and PPIase domains in its N terminus (amino acids 1–38) and C terminus (amino acids 39–163), respectively. To identify the domain of Pin1 responsible for the association with CRTC2, we prepared GST-Pin1, the GST-Pin1 WW domain, and the GST-Pin1 PPIase domain. These GST proteins were conjugated to beads, followed by incubation with cell lysates from MEF-tagged CRTC2 overexpressing HepG2 cells. GST-Pin1 but not GST alone bound to CRTC2 *in vitro* (Fig. 1*E*). Using this pull-down system, it was shown that the GST-WW domain, but not the GST-PPIase domain, binds to CRTC2 (Fig. 1*F*). In addition, okadaic acid treatment significantly increased the association of CRTC2 with Pin1 (Fig. 1*G*),

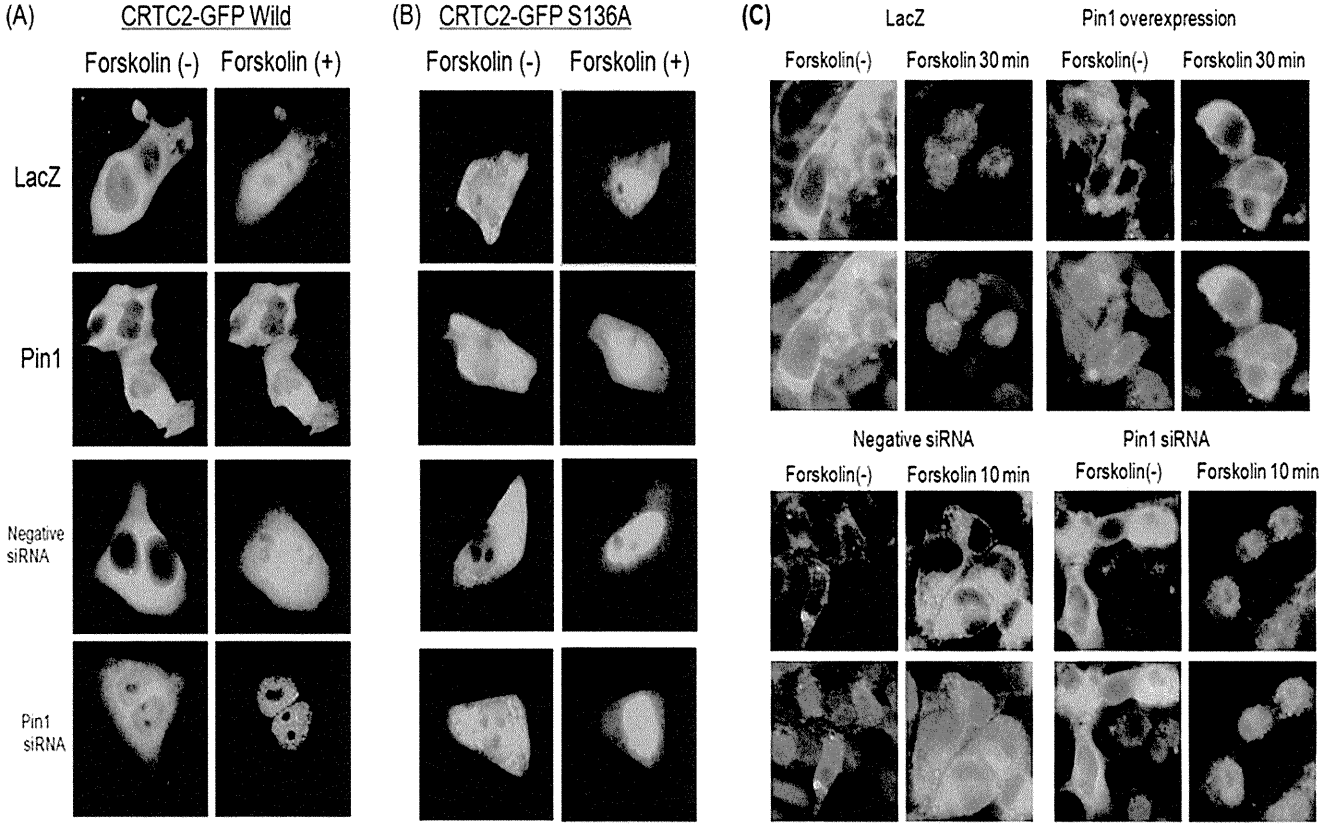

FIGURE 3. **Effect of Pin1 on subcellular localization of GFP-tagged CRTC2.** *A* and *B*, LacZ or Pin1 was overexpressed, or HepG2 cells were treated with control or Pin1 siRNAs. Then GFP-tagged CRTC2 was overexpressed in HepG2 cells. These cells were treated with forskolin, and the subcellular localization of GFP-tagged wild type or S136A CRTC2 was examined at the indicated periods after initiating forskolin stimulation. Representative data from four independent experiments are shown. *C*, LacZ or Pin1 was overexpressed in HepG2 cells, or the cells were treated with control or Pin1 siRNAs. These cells were treated with forskolin, and the subcellular localization of endogenous CRTC2 was determined by immunostaining at 10 or 30 min after initiating forskolin stimulation. Nuclei were stained with DAPI. Representative data from five independent experiments are shown.

suggesting the involvement of serine and/or threonine phosphorylation(s) in CRTC2.

Pin1 Associates with Ser^{136}-containing Motif in the NLS Domain of CRTC2—Subsequently, to reveal the domain of CRTC2 responsible for the association with Pin1, six Ds-Red-tagged CRTC2 N terminus deletion mutants (Fig. 2*A*) and GFP-tagged Pin1 were simultaneously overexpressed in Sf9 cells. As shown in Fig. 2*B*, CRTC2 deletion mutant 2 (D-2), containing amino acids 121–238, was immunoprecipitated with GFP-tagged Pin1 but not with GFP alone. This portion contains three serine-proline motifs (Fig. 2*C*). Each of these serine residues was replaced with alanine, creating a mutant that did not associate with Pin1. As shown in Fig. 2*D*, CRTC2 with serine 136 replaced by alanine did not bind to Pin1, whereas CRTC with serine 129 or 131 bound to Pin1 (data not shown). These observations indicated that the association between CRTC2 and Pin1 is mediated via the phosphoserine 136-containing motif in CRTC2 and the WW domain in Pin1. Ser^{136} is in the NLS domain, and a high level of Ser^{136} phosphorylation was demonstrated in a previous report (16).

Pin1 Inhibits CRTC2 Translocation from the Cytosol to the Nucleus—To test whether or not the effect of Pin1 on CRE transcriptional activity is mediated via the effect on the subcellular localization of CRTC2, the GFP-tagged CRTC2 was overexpressed, and the effects of the Pin1 expression level on the subcellular localization of GFP-tagged CRTC2 were analyzed in the absence or presence of forskolin stimulation (Fig. 3*A*). In the control LacZ-overexpressing or control siRNA-treated HepG2 cells, GFP-tagged CRTC2 was translocated from the cytosol to the nucleus, as reported previously (9). Pin1 overexpression markedly inhibited forskolin-induced translocation of CRTC2 into the nucleus. In addition, gene silencing of Pin1 using siRNA markedly enhanced the nuclear translocation of Pin1 in comparison with treatment with control siRNA. Although nuclear CRTC2 S136A (unable to bind to Pin1) was required for forskolin stimulation, it had no effect on either Pin1 overexpression or Pin1 siRNA (Fig. 3*B*).

In addition, we investigated the effect of Pin1 on the distribution of CRTC2 S171A. CRTC2 S171A (unable to bind to 14-3-3) was mainly present in the nucleus regardless of forskolin stimulation (supplemental Fig. 2). Pin1 overexpression slightly increased CRTC2 S171A in the cytosol, whereas Pin1 siRNA treatment reduced the amount of CRTC2 S171A in the cytosol. This effect of Pin1 was essentially in agreement with the results obtained for wild-type CRTC2.

Similar results were obtained by immunostaining the endogenous CRTC2 in HepG2 cells (Fig. 3*C*). Pin1 overexpression attenuated the forskolin-induced nuclear translocation of CRTC2 as compared with LacZ overexpression. On the other hand, treatment with Pin1 siRNA increased CRTC2 in the nucleus under forskolin stimulation as compared with the control siRNA.

Neither the distribution nor the expression of Pin1 was changed by forskolin or insulin stimulation (supplemental Fig. 3). Thus, a change in Pin1 is not required for regulation of the CRTC2 distribution.

Pin1 Associates with CRTC1 and Induces Its Localization in the Cytosol—The CRTC family consists of three isoforms, CRTC1, CRTC2, and CRTC3. The motif of CRTC2 responsible for the association with Pin1 is present in the NLS and is conserved in CRTC1 but not in CRTC3 (supplemental Fig. 4*A*). Thus, the associations of Pin1 with CRTC1 were also investigated using HepG2 cells. As shown in supplemental Fig. 4*B*, FLAG-tagged CRTC1 was detected in anti-GFP immunoprecipitates from the cells expressing GFP-tagged Pin1 and FLAG-tagged CRTC1. As shown in supplemental Fig. 4*C*, FLAG-tagged CRTC1, in which serine 155 is replaced with alanine, did not bind to GFP-tagged Pin1, unlike the FLAG-tagged wild-type CRTC1.

Then the effects of Pin1 on localizations of CRTC1 were examined. When LacZ was overexpressed, GFP-tagged CRTC1 was present in the cytosol and translocated to the nucleus in response to forskolin stimulation (supplemental Fig. 4*D*). This translocation was markedly inhibited by Pin1 overexpression (supplemental Fig. 4*D*).

CRTC2 Associated with Pin1 Did Not Bind to CREB—Formation of the CREB·CBP·CTRC complex, which binds to a CRE site, is critical for CRE transcriptional activation. We investigated whether or not the CREB·CBP·CRTC2·Pin1 complex can form, using the baculovirus and Sf9 cell overexpression system. When CRTC2 and CREB were both overexpressed in HepG2 or Sf9 cells, CREB was detected in the CRTC2 immunoprecipitate. Interestingly, the overexpression of Pin1 markedly reduced the association between CREB and CRTC2, in either HepG2 or Sf9 cells (Fig. 4, *A* and *B*).

Furthermore, the effect of Pin1 on the association between CRTC2 and 14-3-3 was investigated. In Sf9 cell lysates overexpressing CREB and CRTC2, both CRTC2 and endogenously expressed 14-3-3 protein were detected in anti-CREB immunoprecipitates (Fig. 4*C*). In the case of triple overexpressions of CRTC2, CREB, and GFP-tagged Pin1, CRTC2 and 14-3-3 were detectable in the GFP-tagged Pin1 immunoprecipitate (Fig. 4*D*).

Similar results were obtained in the HepG2 cells. The association between MEF-tagged CRTC2 and endogenously expressed 14-3-3 was not affected by the overexpression of Pin1 (supplemental Fig. 5*A*). In addition, Pin1 overexpression did not affect the phosphorylation level of Ser^{171}, responsible for the association with 14-3-3, in either basal or forskolin-stimulated conditions (supplemental Fig. 5*B*). These results suggest that Pin1-associated CRTC2 is capable of binding to 14-3-3 protein but not to CREB.

Pin1 Inhibits CRE Transcriptional Activity and Its Downstream PEPCK Expression—Subsequently, to elucidate the role of Pin1 in CRE transcriptional activity, the effects of Pin1 overexpression and Pin1 gene silencing using siRNA on the CRE and PEPCK luciferase assay, and PEPCK mRNA level were investigated in HepG2 cells (Fig. 5). The amount of overexpressed Pin1 was ~5 times that of endogenous Pin1 in HepG2 cells. Under these conditions, forskolin-induced transcriptional activity and PEPCK mRNA induction were significantly attenuated (Fig. 5, *A–C*). On the contrary, gene suppression of Pin1 using siRNA significantly enhanced these events (Fig. 5, *D–F*). In addition, suppressions of CRE-luciferase and PEPCK-luciferase activities by Pin1 overexpression were observed in immortalized human hepatocytes (supplemental Fig. 6) (25), suggesting that this mechanism is independent of the glucose sensitivity of the cell type. An inhibitory effect of Pin1 on CRE luciferase activity was observed when wild type or S171A CRTC2, but not S136A, was overexpressed, consistent with the results showing Pin1 to regulate the translocation of CRTC2 (supplemental Fig. 7). Thus, the Pin1 expression level was revealed to negatively regulate CRE transcriptional activity.

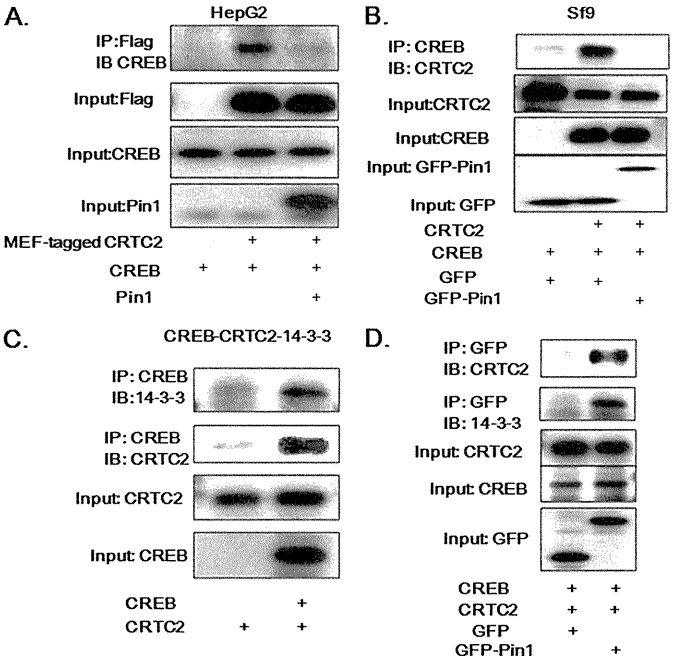

FIGURE 4. **Binding of Pin1 to CRTC2 inhibits the association between CREB and CRTC2 but not that between 14-3-3 and CRTC2.** *A*, MEF-tagged CRTC2, CREB, and Pin1 were overexpressed in HepG2 cells in the indicated combinations. The cell lysates were immunoprecipitated (*IP*) with anti-FLAG antibody and immunoblotted (*IB*) with anti-CREB antibody. *B*, CRTC2, CREB, and Pin1 were overexpressed in Sf9 cells in the indicated combinations. The cell lysates were immunoprecipitated with anti-CREB antibody and immunoblotted with anti-CRTC2 antibody. *C*, CREB and CRTC2 were overexpressed in Sf9 cells. The cell lysates were immunoprecipitated with anti-CREB antibody and immunoblotted with anti-14-3-3 protein antibody. *D*, CREB, CRTC2, and either GFP or GFP-Pin1 were overexpressed in Sf9 cells. The cell lysates were immunoprecipitated with anti-GFP antibody and immunoblotted with anti-CRTC2 or anti-14-3-3 protein antibody. Representative data from four independent experiments are shown.

Chromatin Immunoprecipitation Assay with Anti-CRTC2 and CREB Antibodies—Because Pin1-associated CRTC2 did not bind CREB, we performed a ChIP assay to investigate whether or not Pin1 affected recruitment of CRTC2 to cAMP-responsive elements upstream of PEPCK, NR4A2, and CGA genes (Fig. 5*G*). The PCR product obtained using the anti-CREB immunoprecipitate was unchanged regardless of forskolin stimulation or Pin1 overexpression. In contrast, the PCR product of the anti-CRTC2 immunoprecipitate was markedly increased by forskolin stimulation, and Pin1 overexpression abolished this increase. Forskolin stimulation induced CBP recruitment to the promoter as well as CRTC2, but Pin1 overexpression had no effect.

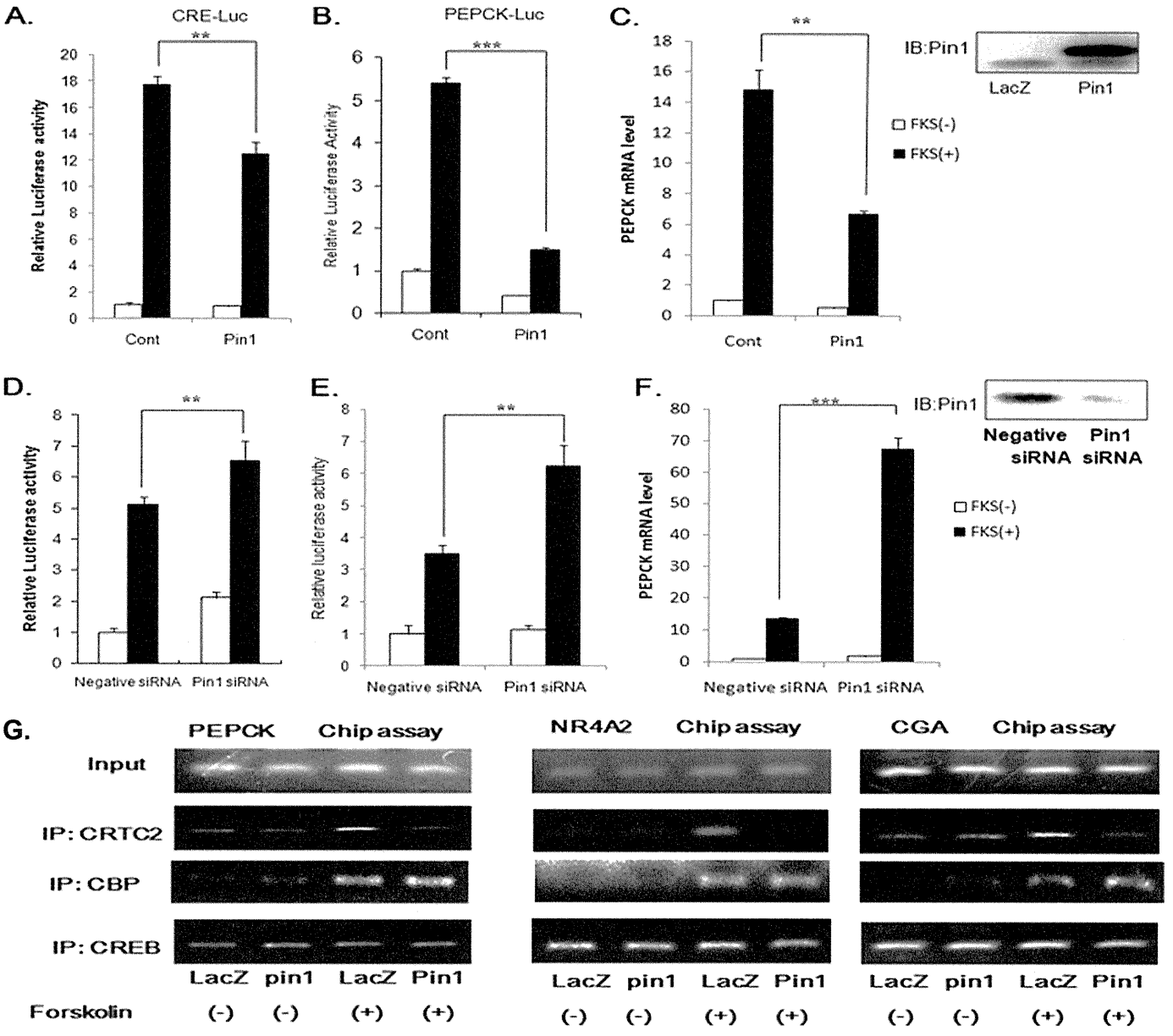

FIGURE 5. **Pin1 suppresses CRE luciferase activity and PEPCK mRNA level in HepG2 cells.** *A* and *B*, LacZ or Pin1 was overexpressed in HepG2 cells transfected with pTAL and pTAL-CRE or pTAL-PEPCK. *D* and *E*, these transfected HepG2 cells were treated with control siRNA or Pin1 siRNA. In two experiments, with and without forskolin stimulation for 6 h, the cell lysates from HepG2 cells were subjected to the luciferase assay. *C* and *F*, PEPCK mRNA levels were also measured. Representative data from four independent experiments are shown. **, $p < 0.01$ *versus* LacZ or negative siRNA. *G*, HepG2 cells overexpressing LacZ or Pin1 were subjected to the CHIP assay using anti-CRTC2, anti-CNP, or anti-CREB antibodies and primers corresponding to the PEPCK, NR4A2, and CGA promoter regions. Representative data from four independent experiments are shown. *IB*, immunoblot; *IP*, immunoprecipitation. *Error bars*, S.E.

Thus, it was suggested that CRTC2 associated with Pin1 was removed from CREB located in the CRE sequence in the PEPCK, NR4A2, and CGA promoter region.

Hepatic Pin1 Overexpression Reduces PEPCK Expression and Decreases Hyperglycemia in STZ-induced Diabetic Mice—CRTC2 is a major transcriptional co-activator for hepatic glucose regulation via its effects on PEPCK expression. Thus, we considered the possibility of the regulation of PEPCK expression by Pin1 in the liver, and an adenovirus expressing Pin1 was introduced into STZ-induced insulin-deficient diabetic mice. Due to the insulin deficiency, as reported previously, hepatic PEPCK mRNA and serum blood glucose levels were markedly increased in fed and fasted state, as compared with the control mice (Fig. 6). The adenovirus for Pin1 expression was injected intravenously, and 96 h later, overexpressed Pin1 was detected only in the liver (Fig. 6*A*) and not in other tissues. With Pin1 overexpression in the liver, the increased hepatic PEPCK mRNA level in STZ-mice was normalized, and blood glucose elevation was also partially but significantly reduced in both the fed and the fasting state (Fig. 6, *B–E*). Pin1 overexpression exerted the same effects on other CRE-dependent transcriptional genes, such as G6Pase, PGC-1a, and CPT-1. These findings revealed Pin1 to be a regulator of CRE-dependent transcriptional genes *in vivo*.

Pin1 Expression Is Low in Fasting State—Finally, we investigated the changes in Pin1 expressions under different nutrient condi-

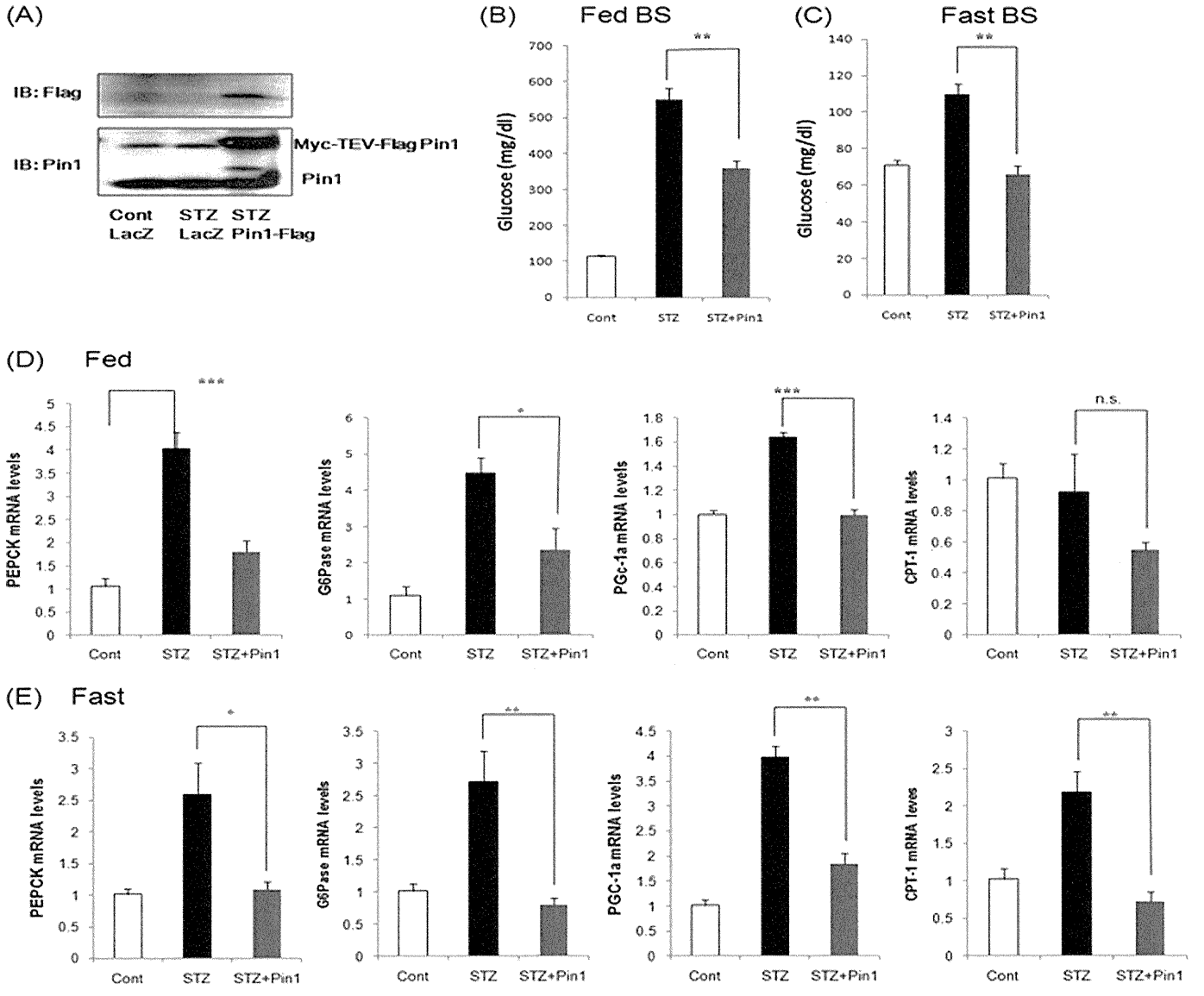

FIGURE 6. **Hepatic overexpression of Pin1 restored elevated CRE-dependent transcriptional genes and hyperglycemia in STZ-treated mice.** STZ-treated diabetic C57BL/6 male mice were injected with 2.5×10^7 plaque-forming units/g body weight of adenovirus containing β-galactosidase (*LacZ*) or FLAG-tagged Pin1 construct via the tail vein. *A*, immunoblotting of hepatic tissue lysates with anti-FLAG or anti-Pin1 antibody. *B* and *C*, serum glucose concentrations in fed and fasting states ($n = 6$, each group). *D* and *E*, CRE-dependent transcriptional gene mRNA levels in the liver. **, $p < 0.01$ *versus* STZ; ***, $p < 0.001$ *versus* STZ. *Error bars*, S.E.

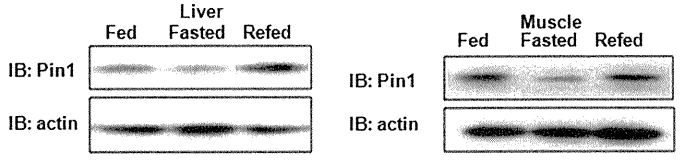

FIGURE 7. **Pin1 expression is regulated by nutrient conditions.** Mice were fed routinely, starved for 20 h, or refed for 4 h after a 20-h fast. Liver (*left*) and muscle (*right*) cell lysates were prepared and then immunoblotted with anti-Pin1 antibody. A representative immunoblot (*IB*) is shown in the *upper panel*.

tions. Interestingly, we found that the Pin1 expression level is low in the fasted state but is increased by feeding (Fig. 7). Thus, Pin1 expression appears to be regulated by nutrient conditions.

DISCUSSION

CRE transcriptional activity is enhanced through association of the CREB·CBP·CRTC complex on a CRE site. The co-activator of CREB termed the CRTC family consists of three isoforms, CRTC1, CRTC2, and CRTC3 (18). CRTC2 was reported to be important for the regulation of CRE transcriptional activity and its downstream PEPCK gene expression (20). Depletion of nuclear CRTC2 leads to the suppression of CRE transcriptional activity (20). Thus, both the subcellular localization of CRTC2 and CREB·CBP·CRTC complex formation are critical for CRE transcriptional activity. CRTC2 is reportedly phosphorylated by AMPK and SIK, and phosphorylated CRTC2 binds to 14-3-3 protein and is thereby shifted from the nucleus to the cytoplasm (21). The Montiminy group (16) has identified 12 independent phosphorylated serine residues on CRTC2 using tandem MS analysis. They demonstrated that PKA inhibits the activity of SIK and reduces Ser^{171} phosphorylation leading to binding with 14-3-3 protein and translocation to the cytosol (16). However, the importance of other phosphorylation sites identified in their study, such as Ser^{136} remains unknown.

Pin1 Binds to CRTC2 and Suppresses CRE Activity

In this study, it was demonstrated that Pin1 associates with the CRTC family of proteins consisting of CRTC1 and CRTC2. Because the portion of CRTC1 and CRTC2 responsible for the association with Pin1 is in the NLS domain, we considered the possibility that the binding of Pin1 to this portion would interrupt NLS function, resulting in their export from the nucleus. In fact, our observations using GFP-tagged CRTC1 and CRTC2 as well as staining of endogenous CRTC2 supported our hypothesis. On the other hand, gene silencing of Pin1 using siRNA markedly induced nuclear localization of CRTC2 when stimulated with forskolin. It is likely that altered localization of CTRC2 due to Pin1 takes place independently of the binding of 14-3-3 protein to CRTC2 because Pin1 overexpression affected neither the Ser^{171} phosphorylation level of CRTC2 nor the association with 14-3-3.

A further interesting issue is that CRTC2 associated with Pin1 did not bind to CREB. This phenomenon cannot be attributable to the different subcellular distributions of CREB, CBP, and CRTC because highly overexpressed CREB, CBP, and CRTC2 are present in the cytosol of Sf9 cells. Taken together, these observations indicate the association of Pin1 with CRTC2 to decrease the nuclear CBP·CRTC2·CREB complex via two mechanisms (*i.e.* the export of CRTC2 and interruption of the association between CRTC2 and CREB). Thus, the Pin1 expression level is a key factor regulating CRE transcriptional activity.

We investigated the effects of various kinase inhibitors on the association between CRTC2 and Pin1, using HepG2 cells, in an effort to identify the kinase that is involved in the phosphorylation of S136A on CRTC2. However, we were unable to obtain clear results. Although we did not discover which kinase(s) phosphorylates the Ser^{136} of CRTC2 responsible for the association with Pin1 in this study, high basal phosphorylation of Ser^{136} was already demonstrated in a previous report (16).

Prior studies have also shown that Pin1 expression generally correlates with cell proliferative potential in normal tissues (1, 26, 27) and is further up-regulated in many human cancers (28–31). In addition, interestingly, we noticed that the amount of Pin1 was higher in the fed than in the fasting state, in both liver and muscle. However, neither insulin nor forskolin has any effect on the expression of Pin1 in HepG2. Thus, the mechanism(s) involved in the altered expression of Pin1 remains unclear, although this is an important issue that merits further investigation.

In the liver, CRE transcriptional activity plays a critical role in gluconeogenesis (32–34). In addition, in the diabetic state, insufficient suppression of CRE transcriptional activity is regarded as a mechanism underlying hyperglycemia under fasted conditions (35). In the present study, our final experiment examined whether Pin1 overexpression might improve the hyperglycemia in insulin-deficient STZ-treated mice. In these mice, gluconeogenic enzymes, such as PEPCK, under the control of CRE transcriptional activity are reportedly up-regulated (20, 36, 37) due to insulin deficiency and the relatively increased effect of glucagon. The fact that Pin1 overexpression reduced the high PEPCK expression and its resultant fasting serum glucose elevation in STZ-treated mice suggests that the Pin1 expression level is involved in regulating glucose metabolism. Thus, an agent affecting Pin1 expression or activity may represent a novel therapeutic strategy for diabetes.

To date, numerous proteins have been identified as substrates of Pin1 (4, 5, 38). With the proline conformational change induced by Pin1, the structure and function of the target protein are modified, which affects protein stabilization, subcellular localization, phosphorylation, transcriptional activity, etc. In the case of CTRC2, both subcellular localization and the complex-forming function with CREB are affected.

Although we did not investigate the physiological effects occurring via CRTC1 induced by the association with Pin1, we did observe that Pin1 is highly expressed in the brain, whereas its enzymatic activity is blunted by oxidative stress modification that occurs in the early stages of Alzheimer disease (39). Although the physiological function of Pin1 in neurons remains largely unknown, numerous reports have implicated CRE transcriptional activity in brain function (40–42). Thus, further important evidence may be obtained from studies of Pin1 and CRTC1 in the brain or other tissues.

In summary, CRTC2 was identified as a new Pin1-binding protein. The CBP·CRTC2·CREB complex promotes gluconeogenesis. Pin1 binding to CRTC2 prevents this complex formation, thereby suppressing CRE transcriptional activity (supplemental Fig. 8). These findings indicate that Pin1 is a regulator of gluconeogenesis and may be a new target for diabetic therapy.

REFERENCES

1. Lu, K. P., Hanes, S. D., and Hunter, T. (1996) *Nature* **380,** 544–547
2. Lu, P. J., Wulf, G., Zhou, X. Z., Davies, P., and Lu, K. P. (1999) *Nature* **399,** 784–788
3. Pinton, P., Rimessi, A., Marchi, S., Orsini, F., Migliaccio, E., Giorgio, M., Contursi, C., Minucci, S., Mantovani, F., Wieckowski, M. R., Del Sal, G., Pelicci, P. G., and Rizzuto, R. (2007) *Science* **315,** 659–663
4. Takahashi, K., Uchida, C., Shin, R. W., Shimazaki, K., and Uchida, T. (2008) *Cell Mol. Life Sci.* **65,** 359–375
5. Wulf, G., Finn, G., Suizu, F., and Lu, K. P. (2005) *Nat. Cell Biol.* **7,** 435–441
6. Ranganathan, R., Lu, K. P., Hunter, T., and Noel, J. P. (1997) *Cell* **89,** 875–886
7. Schutkowski, M., Bernhardt, A., Zhou, X. Z., Shen, M., Reimer, U., Rahfeld, J. U., Lu, K. P., and Fischer, G. (1998) *Biochemistry* **37,** 5566–5575
8. Bittinger, M. A., McWhinnie, E., Meltzer, J., Iourgenko, V., Latario, B., Liu, X., Chen, C. H., Song, C., Garza, D., and Labow, M. (2004) *Curr. Biol.* **14,** 2156–2161
9. Dentin, R., Hedrick, S., Xie, J., Yates, J., 3rd, and Montminy, M. (2008) *Science* **319,** 1402–1405
10. He, L., Sabet, A., Djedjos, S., Miller, R., Sun, X., Hussain, M. A., Radovick, S., and Wondisford, F. E. (2009) *Cell* **137,** 635–646
11. Herzig, S., Long, F., Jhala, U. S., Hedrick, S., Quinn, R., Bauer, A., Rudolph, D., Schutz, G., Yoon, C., Puigserver, P., Spiegelman, B., and Montminy, M. (2001) *Nature* **413,** 179–183
12. Jansson, D., Ng, A. C., Fu, A., Depatie, C., Al Azzabi, M., and Screaton, R. A. (2008) *Proc. Natl. Acad. Sci. U.S.A.* **105,** 10161–10166
13. Lerner, R. G., Depatie, C., Rutter, G. A., Screaton, R. A., and Balthasar, N. (2009) *EMBO Rep.* **10,** 1175–1181
14. Liu, Y., Dentin, R., Chen, D., Hedrick, S., Ravnskjaer, K., Schenk, S., Milne, J., Meyers, D. J., Cole, P., Yates, J., 3rd, Olefsky, J., Guarente, L., and Montminy, M. (2008) *Nature* **456,** 269–273
15. Radhakrishnan, I., Pérez-Alvarado, G. C., Parker, D., Dyson, H. J., Montminy, M. R., and Wright, P. E. (1997) *Cell* **91,** 741–752
16. Screaton, R. A., Conkright, M. D., Katoh, Y., Best, J. L., Canettieri, G., Jeffries, S., Guzman, E., Niessen, S., Yates, J. R., 3rd, Takemori, H., Okamoto, M., and Montminy, M. (2004) *Cell* **119,** 61–74

17. Zhou, X. Y., Shibusawa, N., Naik, K., Porras, D., Temple, K., Ou, H., Kaihara, K., Roe, M. W., Brady, M. J., and Wondisford, F. E. (2004) *Nat. Med.* **10,** 633–637
18. Iourgenko, V., Zhang, W., Mickanin, C., Daly, I., Jiang, C., Hexham, J. M., Orth, A. P., Miraglia, L., Meltzer, J., Garza, D., Chirn, G. W., McWhinnie, E., Cohen, D., Skelton, J., Terry, R., Yu, Y., Bodian, D., Buxton, F. P., Zhu, J., Song, C., and Labow, M. A. (2003) *Proc. Natl. Acad. Sci. U.S.A.* **100,** 12147–12152
19. Wu, Z., Huang, X., Feng, Y., Handschin, C., Feng, Y., Gullicksen, P. S., Bare, O., Labow, M., Spiegelman, B., and Stevenson, S. C. (2006) *Proc. Natl. Acad. Sci. U.S.A.* **103,** 14379–14384
20. Dentin, R., Liu, Y., Koo, S. H., Hedrick, S., Vargas, T., Heredia, J., Yates, J., 3rd, and Montminy, M. (2007) *Nature* **449,** 366–369
21. Koo, S. H., Flechner, L., Qi, L., Zhang, X., Screaton, R. A., Jeffries, S., Hedrick, S., Xu, W., Boussouar, F., Brindle, P., Takemori, H., and Montminy, M. (2005) *Nature* **437,** 1109–1111
22. Sakoda, H., Gotoh, Y., Katagiri, H., Kurokawa, M., Ono, H., Onishi, Y., Anai, M., Ogihara, T., Fujishiro, M., Fukushima, Y., Abe, M., Shojima, N., Kikuchi, M., Oka, Y., Hirai, H., and Asano, T. (2003) *J. Biol. Chem.* **278,** 25802–25807
23. Xu, Y. X., and Manley, J. L. (2007) *Genes Dev.* **21,** 2950–2962
24. Shen, Z. J., Esnault, S., Schinzel, A., Borner, C., and Malter, J. S. (2009) *Nat. Immunol.* **10,** 257–265
25. Tontonoz, P., Hu, E., Devine, J., Beale, E. G., and Spiegelman, B. M. (1995) *Mol. Cell. Biol.* **15,** 351–357
26. Waki, K., Anno, K., Ono, T., Ide, T., Chayama, K., and Tahara, H. (2010) *Cancer Sci.* **101,** 1678–1685
27. Winkler, K. E., Swenson, K. I., Kornbluth, S., and Means, A. R. (2000) *Science* **287,** 1644–1647
28. Ryo, A., Nakamura, M., Wulf, G., Liou, Y. C., and Lu, K. P. (2001) *Nat. Cell Biol.* **3,** 793–801
29. Wulf, G. M., Ryo, A., Wulf, G. G., Lee, S. W., Niu, T., Petkova, V., and Lu, K. P. (2001) *EMBO J.* **20,** 3459–3472
30. Yeh, E., Cunningham, M., Arnold, H., Chasse, D., Monteith, T., Ivaldi, G., Hahn, W. C., Stukenberg, P. T., Shenolikar, S., Uchida, T., Counter, C. M., Nevins, J. R., Means, A. R., and Sears, R. (2004) *Nat. Cell Biol.* **6,** 308–318
31. Zheng, H., You, H., Zhou, X. Z., Murray, S. A., Uchida, T., Wulf, G., Gu, L., Tang, X., Lu, K. P., and Xiao, Z. X. (2002) *Nature* **419,** 849–853
32. Erion, D. M., Ignatova, I. D., Yonemitsu, S., Nagai, Y., Chatterjee, P., Weismann, D., Hsiao, J. J., Zhang, D., Iwasaki, T., Stark, R., Flannery, C., Kahn, M., Carmean, C. M., Yu, X. X., Murray, S. F., Bhanot, S., Monia, B. P., Cline, G. W., Samuel, V. T., and Shulman, G. I. (2009) *Cell Metab.* **10,** 499–506
33. Rhee, J., Inoue, Y., Yoon, J. C., Puigserver, P., Fan, M., Gonzalez, F. J., and Spiegelman, B. M. (2003) *Proc. Natl. Acad. Sci. U.S.A.* **100,** 4012–4017
34. Rodgers, J. T., Lerin, C., Haas, W., Gygi, S. P., Spiegelman, B. M., and Puigserver, P. (2005) *Nature* **434,** 113–118
35. Yoon, J. C., Puigserver, P., Chen, G., Donovan, J., Wu, Z., Rhee, J., Adelmant, G., Stafford, J., Kahn, C. R., Granner, D. K., Newgard, C. B., and Spiegelman, B. M. (2001) *Nature* **413,** 131–138
36. Clément, S., Krause, U., Desmedt, F., Tanti, J. F., Behrends, J., Pesesse, X., Sasaki, T., Penninger, J., Doherty, M., Malaisse, W., Dumont, J. E., Le Marchand-Brustel, Y., Erneux, C., Hue, L., and Schurmans, S. (2001) *Nature* **409,** 92–97
37. Fisher, S. J., and Kahn, C. R. (2003) *J. Clin. Invest.* **111,** 463–468
38. Ryo, A., Suizu, F., Yoshida, Y., Perrem, K., Liou, Y. C., Wulf, G., Rottapel, R., Yamaoka, S., and Lu, K. P. (2003) *Mol Cell.* **12,** 1413–1426
39. Sultana, R., Boyd-Kimball, D., Poon, H. F., Cai, J., Pierce, W. M., Klein, J. B., Markesbery, W. R., Zhou, X. Z., Lu, K. P., and Butterfield, D. A. (2006) *Neurobiol. Aging* **27,** 918–925
40. Bito, H., Deisseroth, K., and Tsien, R. W. (1996) *Cell* **87,** 1203–1214
41. Nibuya, M., Nestler, E. J., and Duman, R. S. (1996) *J. Neurosci.* **16,** 2365–2372
42. Tao, X., Finkbeiner, S., Arnold, D. B., Shaywitz, A. J., and Greenberg, M. E. (1998) *Neuron* **20,** 709–726

The Journal of Nutrition
Nutrition and Disease

Dietary Fiber Intake Is Associated with Reduced Risk of Mortality from Cardiovascular Disease among Japanese Men and Women[1–3]

Ehab S. Eshak,[4] Hiroyasu Iso,[4]* Chigusa Date,[5] Shogo Kikuchi,[6] Yoshiyuki Watanabe,[7] Yasuhiko Wada,[8] Kenji Wakai,[9] Akiko Tamakoshi,[6] and the JACC Study Group[10]

[4]Public Health, Department of Social and Environmental Medicine, Osaka University Graduate School of Medicine, Yamadoka, 2-2 Suita-shi, Osaka, Japan 565-0871; [5]Department of Food Science and Nutrition, Faculty of Human Life and Environment, Nara Women's University, Kitauoya Nishimachi, Nara, Japan 630-8506; [6]Department of Public Health, Aichi Medical University School of Medicine, Nagakute, Aichi, Japan 480-1195; [7]Department of Epidemiology for Community Health and Medicine, Kyoto Prefectural University of Medicine Graduate School of Medical Sciences, Kajii-cho,Kawaramachi- Hirokoji, Kamigyo-ku, Kyoto, Japan 602-8566; [8]Department of Health Science, Faculty of Human Life and Environmental Science, Kochi Women's University, Eikokuji-cho, 5-15 Kochi-shi, Japan 780-8515; and [9]Department of Health and Community Medicine, Graduate School of Medicine, Nagoya University, 65 Tsurumai-cho, Shwa-Ku, Nagoya, Japan 466-8550

Abstract

Dietary fiber protects against coronary heart disease (CHD), but evidence in Asia is limited. We examined the association between dietary fiber intake and mortality from cardiovascular disease (CVD) in a Japanese population in a prospective study of 58,730 Japanese men and women aged 40–79 y in which dietary fiber intake was determined by a self-administered FFQ. The participants were followed up from 1988–1990 to the end of 2003. Hazard ratios (HR) and 95% CI of mortality were calculated per quintile of fiber intake. During the 14-y follow-up, a total of 2080 CVD deaths (983 strokes, 422 CHD, and 675 other CVD) were documented. Total, insoluble, and soluble dietary fiber intakes were inversely associated with risk of mortality from CHD and total CVD for both men and women. For men, the multivariable HR (95% CI) for CHD in the highest vs. the lowest quintiles were 0.81 [(95% CI, 0.61–1.09); P-trend = 0.02], 0.48 [(95% CI, 0.27–0.84); P-trend < 0.001], and 0.71 [(95% CI, 0.41–0.97); P-trend = 0.04] for total, insoluble, and soluble fiber, respectively. The respective HR (95% CI) for women were 0.80 [(95% CI, 0.57–0.97); P-trend = 0.01], 0.49 [(95% CI, 0.27–0.86); P-trend = 0.004], and 0.72 [(95% CI, 0.34–0.99); P-trend = 0.03], respectively. For fiber sources, intakes of fruit and cereal fibers but not vegetable fiber were inversely associated with risk of mortality from CHD. In conclusion, dietary intakes of fiber, both insoluble and soluble fibers, and especially fruit and cereal fibers, may reduce risk of mortality from CHD. J. Nutr. 140: 1445–1453, 2010.

Introduction

The WHO defines dietary fiber as the edible parts of plants or analogous carbohydrates that are resistant to digestion and absorption in human small intestine and undergoes complete or partial fermentation in large intestine (1). Burkitt and Trowell

[1] Supported by grants-in-aid for scientific research from the Ministry of Education, Science, Sports and Culture of Japan (Monbusho) (61010076, 62010074, 63010074, 1010068, 2151065, 3151064, 4151063, 5151069, 6279102, 11181101, 17015022, and 18014011) to the Japan Collaborative Cohort (JACC) Study.

[2] Author disclosures:-Eshak S. Ehab, Iso Hiroyasu, Date Chigusa, Kikuchi Shogo, Tamakoshi Akiko, Watanabe Yoshiyuki, Wada Yasuhiko, Wakai Kenji, and JACC Study Group, no conflict of interest.

[3] Supplemental Tables 1–3 are available with the online posting of this paper at jn.nutrition.org.

[10] The members of the JACC Study Group are as follows: Dr. Akiko Tamakoshi (present chairperson of the study group), Aichi Medical University School of Medicine; Mitsuru Mori and Fumio Sakauchi, Sapporo Medical University School of Medicine, Japan; Yutaka Motohashi, Akita University School of Medicine, Japan; Ichiro Tsuji, Tohoku University Graduate School of Medicine, Japan; Yosikazu Nakamura, Jichi Medical School, Japan; Hiroyasu Iso, Osaka University School of Medicine, Japan; Haruo Mikami, Chiba Cancer Center, Japan; Michiko Kurosawa, Juntendo University School of Medicine, Japan; Yoshiharu Hoshiyama, University of Human Arts and Sciences, Japan; Naohito Tanabe, Niigata University School of Medicine, Japan; Koji Tamakoshi, Nagoya University School of Medicine, Japan; Kenji Wakai, Nagoya University Graduate School of Medicine, Japan; Shinkan Tokudome, Nagoya City University Graduate School of Medical Sciences, Japan; Koji Suzuki, Fujita Health University School of Health Sciences, Japan, Shuji Hashimoto, Fujita Health University School of Medicine, Japan; Shogo Kikuchi, Aichi Medical University School of Medicine, Japan; Yasuhiko Wada, Kansai Rosai Hospital, Japan; Takashi Kawamura, Kyoto University Center for Student Health, Japan; Yoshiyuki Watanabe, Kyoto Prefectural University of Medicine Graduate School of Medical Science, Japan; Kotarou Ozasa, Hiroshima Laboratory, Radiation Effects Research Foundation; Tsuneharu Miki, Kyoto Prefectural University of Medicine Graduate School of Medical Science, Japan; Chigusa Date, Faculty of Human Environmental Sciences, Nara Women's University, Japan; Kiyomi Sakata, Iwate Medical University, Japan; Yoichi Kurozawa, Tottori University Faculty of Medicine, Japan; Takesumi Yoshimura, Fukuoka Institute of Health and Environmental Sciences, Japan; Yoshihisa Fujino, University of Occupational and Environmental Health, Japan; Akira Shibata, Kurume University School of Medicine, Japan; Naoyuki Okamoto, Kanagawa Cancer Center, Japan; Hideo Shio, Moriyama Municipal Hospital, Japan.

* To whom correspondence should be addressed. E-mail: fvgh5640@mb.infoweb.ne.jp or iso@pbhel.med.osaka-u.ac.jp.

Manuscript received February 8, 2010. Initial review completed March 18, 2010. Revision accepted May 24, 2010.
First published online June 23, 2010; doi:10.3945/jn.110.122358.

(2) stated that high dietary fiber intake may protect against chronic diseases; although their hypothesis initially focused on gastrointestinal diseases, it was later expanded to involve cardiovascular diseases (CVD).[11]

Reports of epidemiologic studies in Western countries have strongly suggested that dietary fiber intake offers protection against coronary heart disease (CHD) (3–9), but evidence has been limited in Asia. The mean daily Japanese dietary fiber intake was 20.5 g/d in 1952 and rapidly declined to ~70% of that level in 1970 (14.9 g/d), with little change thereafter (10,11). Meanwhile, during this period without declination of dietary fiber intake between 1970 and 1992, the age-adjusted mortality rates from CHD declined 50% for men and 65% for women (12) and have continued to decline (12,13). Nevertheless, the mean daily Japanese dietary fiber intake is similar to that of some Western countries (3,6) and lower than that of others (4,5,7–9). Therefore, it is worthwhile to investigate whether dietary fibers of different types and sources may protect against CHD with or without a threshold in a Japanese population.

Participants and Methods

Study population. The Japan Collaborative Cohort Study for Evaluation of Cancer Risks, a large prospective study sponsored by the Ministry of Education, Sports and Science, was carried out between 1988 and 1990 and covered a total of 110,792 participants (46,465 male and 64,327 female) aged 40–79 y. Participants were enrolled from 45 study areas throughout Japan, mostly from the general population or those who had undergone municipal health check-ups and completed self-administered questionnaires covering lifestyle data and medical histories of previous CVD and cancer at baseline. A subsample of 39,393 cohort participants donated a residual serum sample that was partitioned into 0.3–0.5-mL aliquots and stored at −80 C° until laboratory analysis. The details of the study procedure were described elsewhere (14,15). In most communities, informed consent was obtained from each participant, except in a few study areas where informed consent was obtained at the community level after the purpose of the study and confidentiality of the data had been explained to community leaders. The ethics committees of the Nagoya University School of Medicine and Osaka University approved the protocol of this investigation.

We excluded 16,109 participants (4683 men and 11,426 women) with a medical history of cancer, stroke, or CHD, and 123 with energy intakes above or below plausible intakes (<500 or >3500 kcal/d = <2096 kJ/d or >14,645 kJ/d). Also, participants whose responses to the FFQ were insufficient, which means failure to give an answer to 5 or more items of the 40 food items of the FFQ, and/or no answer for current rice intake, and/or no answer for current miso soup intake, and/or no answer for current alcohol consumption were excluded. A total of 58,730 (23,119 men and 35,611 women) were eligible for the study.

Mortality surveillance. For mortality surveillance in each of the communities, investigators conducted a systematic review of death certificates, all of which had been forwarded to the public health center in the area of residency. Mortality data were then centralized at the Ministry of Health and Welfare and the underlying causes of death were coded according to the National Vital Statistics system, which is based on the International Classification of Diseases, 10th revised edition.

Participants who died after they had moved from their original communities were treated as censored cases. Of the total 58,730 participants, 2487 (4.2%) moved. Cause-specific mortality was categorized as stroke (I60–I69), CHD (I20–I25), other CVD (I30–I52), and total CVD (I01–I99). The follow-up of mortality was conducted until the end of 2003, except for 4 communities, where follow-up was terminated at the end of 1999.

Diet and baseline survey. A self-administered questionnaire, which included a FFQ, was used to collect the baseline data for demographic characteristics; history of hypertension, diabetes mellitus, and other chronic diseases; family history of cancer; and height and weight, as well as habits related to smoking, alcohol consumption, exercise, and diet.

The FFQ representing the dietary component of the survey included 40 food items (15). Participants were asked about average intake frequency without specifying portion size. There were 5 response choices: almost never, once or twice/mo, once or twice/wk, 3–4 times/wk, and almost every day. Food and nutrient intakes were computed using the Japanese food composition table (4th revised edition) (16) and standard portion sizes derived from weighted dietary records (DR). The details of the study procedure were described elsewhere (14,15). Key's score was calculated using this formula: Key's score = 1.35 [2energy from SFA (% energy) − energy from PUFA (% energy)] + 1.52 [cholesterol intake (mg/1000kcal)][2] (17). Values for total dietary fiber (TDF), insoluble dietary fiber (IDF), and soluble dietary fiber (SDF), obtained by enzymatic-gravimetric methods by Prosky et al. (18), and were derived from the food composition table. The FFQ was validated by using 4 3-d weighed DR over a 1-y period as a reference standard (19). The authors reanalyzed data from the validation study to take into account skewed distributions of nutrient intakes and within-person variations for intake (20). The deattenuated correlation coefficients for energy-adjusted intakes between the FFQ and DR were 0.46 for TDF, 0.47 for IDF, 0.42 for SDF, 0.30 for cereal fiber, 0.33 for fruit fiber, and 0.41 for vegetable fiber ($P < 0.001$ for all). The ratios of mean intakes estimated by the FFQ to those calculated from the DR were 0.60, 0.58, 0.51, 0.66, 0.84, and 0.53 for total, insoluble, soluble, cereal, fruit, and vegetable fibers, respectively.

Statistical analysis. Total, insoluble, soluble, cereal, fruit, and vegetable dietary fiber intakes were calorie adjusted by using the residual method (21) and modeled as categorical (5 quintile groups) variables in the primary analysis. Statistical analyses were based on sex-specific mortality rates of disease outcomes during the follow-up period from 1988–1990 to 2003 (until 1999 for 4 areas). The person-years of the follow-up were calculated from the date of completing the baseline questionnaire to death, moving out of the community, or the end of follow-up, whichever came first.

Because most of distributions for the dietary variables are skewed, sex-specific medians with interquartile range or proportions of cardiovascular risk factors were calculated. The sex-specific hazard ratios (HR) with 95% CI for mortality by disease outcome (stroke, CHD, other CVD, and total CVD) were calculated with reference to the risk according to energy-adjusted total, insoluble, soluble, and different sources of fiber intakes. For Cox proportional hazard models, the PHREG procedure of SAS/STAT software (version 9.1; SAS Institute) was used. There was no evidence that proportional hazards assumptions were violated, as indicated by the lack of significant interaction between the predictors and a function of survival time in the model. The estimates were presented as age-adjusted and multivariable-adjusted models including other potential confounding factors: history of hypertension, history of diabetes, BMI (sex-specific quintiles), smoking status (never, ex-smoker, current smoker of 1–19, and ≥20 cigarettes/d), alcohol consumption (nondrinker, ex-drinker, current drinker of 0.1–22.9, 23.0–45.9, 46.0–68.9, and ≥69.0 g ethanol/d), hours of exercise (almost never, 1–2, 3–4 and ≥5 h/wk), hours of walking (almost never, 0.5, 0.6–0.9, and ≥1 h/d), perceived mental stress (low, moderate, and high), education level (primary school, junior high school, high school, and college or higher), sleep duration (≤6 h, 6–<7 h, 7–<8 h, 8–>9 h, ≥9 h/d), fish, sodium, SFA, (n-3) fatty acids, folic acid, and vitamin E intakes (sex-specific energy-adjusted quintiles), and total energy intake. Because of the high correlations between soluble and insoluble fibers ($r = 0.96$ for men and 0.95 women), they could not be distinguished in the multivariate analysis

Because of low to moderate correlations between different sources of fibers (cereal, fruit, and vegetables), a 3rd model was added for each with further adjustment for intakes of other sources of fiber: for men, $r = -0.31$ between cereal and fruit fibers, −0.43 between cereal and

[11] Abbreviations used: CHD, coronary heart disease; CVD, cardiovascular disease; DR, dietary record; HR, hazard ratio; IDF, insoluble dietary fiber; SDF, soluble dietary fiber; TDF, total dietary fiber.

vegetable fibers, and 0.29 between fruit and vegetable fibers, and for women, $r = -0.33$ between cereal and fruit fibers, −0.43 between cereal and vegetable fibers, and 0.20 between fruit and vegetable fibers. For tests for linear trends across increasing categories of fiber, the categories were treated as a continuous variable and the median intake for the category was designated as its value. All statistical testing were 2-sided, and for all tests $P < 0.05$ was considered significant.

Results

Among the 58,730 adults aged 40–79 y at baseline examination, 2080 total CVD deaths were recorded during the 14.3 y of follow-up, comprising 983 deaths from stroke, 422 from CHD, and 675 from other CVD.

At baseline, both men and women with higher TDF intake were ~6–9 y older, with higher BMI, more educated, more likely to practice sports and to walk, less likely to drink, less likely to be current smokers, and less likely to have a history of hypertension. Furthermore, higher TDF intake was positively associated with higher intakes of fish, vegetables, fruit, meat, milk/dairy, soy, calcium sodium, potassium, vitamin B-6, isoflavones, (n-3) fatty acids, SFA, monounsaturated fatty acid, and PUFA, dietary cholesterol, and the Key's score (**Table 1**).

As for the serum chemistry in the subsample of men ($n = 6767$) and women ($n = 13,102$), higher TDF intake was inversely associated with serum total cholesterol and triglycerides. Similar trends were observed for SDF and IDF (results not shown). There was an ~0.8- to 1.1-fold greater median TDF intake in the highest compared with the lowest quintiles of TDF for men and women.

Sex-specific, age-adjusted mortality from CVD and total CVD was lower for both men and women with higher TDF intake. After adjustment for cardiovascular risk factors and fish, sodium, SFA, (n-3) fatty acid, folate, vitamin E, and total energy intakes, this tendency toward lower mortality was slightly attenuated but remained significant. The multivariable HR of CHD in the highest compared with lowest quintiles were 0.81 [(95% CI, 0.61–1.09); P-trend = 0.02] for men, 0.80 [(95% CI, 0.57–0.97); P-trend = 0.01] for women, and 0.79 [(95% CI, 0.61–0.98); P-trend = 0.01] overall when men and women were combined adjusting for sex (**Supplemental Table 1**). The multivariable HR of total CVD in the highest compared with lowest quintiles were 0.83 [(95% CI, 0.63–1.09); P-trend = 0.05] for men, 0.82 [(95% CI, 0.57–0.97); P-trend = 0.04] for women, and 0.82 [(95% CI, 0.60–0.99); P-trend = 0.02] overall (Supplemental Table 1). There were no significant associations of TDF intake with risk of mortality from stroke or other CVD for either sex (**Table 2**).

After dividing TDF into IDF and SDF, the age-adjusted risks of mortality from CHD and total CVD were lower for both men and women with higher IDF intake (**Table 3**). After adjustment for cardiovascular risk factors and dietary variables, the multivariable HR for mortality from CHD in the highest compared with lowest quintiles of IDF intake were 0.48 [(95% CI, 0.27–0.84); P-trend < 0.001] for men, 0.49 [(95% CI, 0.27–0.86); P-trend = 0.004] for women, and 0.46 [(95% CI, 0.30–0.85); P-trend = <0.001] overall (**Supplemental Table 2**). For mortality from total CVD, the multivariable HR were 0.82 [(95% CI, 0.65–0.98); P-trend = 0.04] for men, 0.69 [(95% CI, 0.53–0.91); P-trend = 0.02] for women, and 0.77 [(95% CI, 0.61–0.96); P-trend = 0.01] overall (Supplemental Table 2). There were no significant associations of IDF intake with risk of mortality from stroke or other CVD for either sex.

Age-adjusted mortality from CHD and total CVD were lower for both men and women with higher SDF intake. The multivariable HR of mortality from CHD in the highest compared with lowest quintiles of SDF intake were 0.71 (0.41–0.97; P-trend = 0.04) for men, 0.72 [(0.34–0.99) P-trend = 0.03] for women, and 0.69 [(0.44–0.94) P-trend = 0.01] overall (Supplemental Table 2). For mortality from total CVD, the multivariable HR were 0.81 [(95% CI, 0.63–1.04); P-trend = 0.04] for men, 0.83 [(95% CI, 0.53–1.02); P-trend = 0.04] for women, and 0.80 [(95% CI, 0.60–0.99); P-trend = 0.02] overall (Supplemental Table 2). There were no significant associations of SDF intake with risk of mortality from stroke or other CVD for either sex.

We analyzed separately the effects of 3 main food sources of dietary fiber (**Table 4; Supplemental Table 3**). Fruit fiber intake was significantly inversely associated with risk of mortality from CHD. The multivariable HR for CHD after further adjusting for other sources of fiber were 0.55 [(95% CI, 0.32–0.96); P-trend = 0.03] for men and 0.42 [(95% CI, 0.33–0.81); P-trend = 0.01] for women. Cereal fiber intake was inversely associated with risk of mortality from CHD; the multivariable HR were 0.89 [(95% CI, 0.65–1.01); P-trend = 0.06] for men and 0.79 [(95% CI, 0.59–0.97); P-trend = 0.04) for women. There was no significant association of vegetable fiber intake with risk of mortality from CHD for either sex.

Discussion

This 14-y prospective study of Japanese men and women aged 40–79 y showed inverse relationships of total, insoluble, soluble, cereal, and fruit fiber intakes and risk of mortality from CHD. These inverse associations were similar for both men and women and stronger for IDF than SDF and for fruit than for cereal fibers.

The inverse associations with mortality from CHD were observed for both IDF and SDF intakes in a pooled analysis of 10 American and European cohort studies (7); HR per 10-g/d increment were 0.80 (95% CI, 0.69–0.92) for IDF and 0.72 (95% CI, 0.55–0.93) for SDF intakes. Further, the somewhat stronger association for IDF than SDF in the present study is consistent with the results of the Health Professionals Follow-up Study (9) and the Iowa Women's Health Study (22). In the Health Professionals Follow-up Study, the multivariable HR of mortality from CHD for each 10-g increment of IDF intake was 0.75 (95% CI, 0.59–0.94) and that of SDF was 1.07 (95% CI, 0.57–2.02). In the Iowa Women's Health Study, the multivariable HR of mortality from CHD in the highest compared with the lowest quintiles was 0.70 [(95% CI, 0.50–0.96); P-trend = 0.05] for IDF and 0.79 [(95% CI, 0.58–1.08); P-trend = 0.30] for SDF.

The inverse associations of fruit and cereal fiber intakes, but not vegetable fiber intake, with mortality from CHD in the present study were consistent with findings from previous studies: the Women's Health study (23), Nurse Health study (24), Cardiovascular Health Study (25), and the pooled analysis of 10 American and European cohort studies (7).

The inverse association between dietary fiber and CHD can be explained by different mechanisms, such as improving blood lipid profile through its cholesterol-lowering effect (26), lowering blood pressure (27) via reduction of abdominal obesity and improvement of vascular reactivity (28), improving insulin sensitivity (29), inhibiting a postprandial rise of glucose and triglycerides (30), and improving fibrinolytic activity (31,32), all of which may prevent or delay the development of atherosclerosis. Previous studies suggested that those effects were derived by both IDF and SDF (7–9,31,33). However, SDF may have a stronger cholesterol-lowering effect (26), whereas IDF may have a stronger clotting factor reduction effect (23,31).

TABLE 1 Cardiovascular risk factors in Japanese men and women according to quintiles of TDF intake at the baseline examination[1]

	Men					Women				
	Q1 (low)	Q2	Q3	Q4	Q5 (high)	Q1 (low)	Q2	Q3	Q4	Q5 (high)
Median intake, *g/d*	6.8	8.7	10.2	11.7	14.0	7.4	9.2	10.50	11.9	13.8
Participants at risk, *n*	4623	4624	4624	4624	4624	7122	7122	7122	7122	7122
Age, *y*	52 (45–60)	55 (47–62)	55 (47–63)	58 (49–64)	60 (52–66)	53 (46–61)	55 (47–62)	56 (48–63)	57 (49–64)	59 (52–66)
BMI, *kg/m²*	22.5 (20.8–24.5)	22.5 (20.8–24.3)	22.6 (20.8–24.4)	22.6 (20.8–24.5)	22.6 (20.8–24.6)	22.7 (20.8–24.8)	22.6 (20.8–24.6)	22.7 (20.8–24.7)	22.8 (20.9–24.8)	22.8 (21.0–24.9)
History of hypertension, %	20	21	20	18	16	18	20	20	21	22
History of diabetes, %	6	6	7	5	6	3	4	3	3	3
Ethanol intake, *g/d*	46 (23–57)	34 (23–46)	23 (17–46)	23 (11–46)	23 (11–46)	7 (3–23)	5 (2–11)	5 (2–11)	5 (2–11)	5 (2–11)
Current smoker, %	62	55	53	52	48	8	6	4	4	3
College or higher education, %	17	18	19	20	19	9	10	11	12	12
High perceived mental stress, %	25	25	25	24	23	23	21	21	20	19
Exercise ≥5h/wk, %	26	30	32	33	35	20	21	23	26	26
Walking ≥1h/d, %	67	67	69	72	73	70	70	72	74	75
Time sleeping, *h*	7.0 (7.0–8.0)	7.0 (7.0–8.0)	7.0 (7.0–8.0)	7.7 (7.0–8.0)	8.0 (7.0–8.0)	7.0 (6.0–8.0)	7.0 (6.0–8.0)	7.0 (6.0–8.0)	7.0 (6.5–8.0)	7.0 (6.5–8.0)
Food group intakes,[2] *g/d*										
Fish	35 (22–56)	39 (25–60)	43 (26–70)	45 (30–72)	57 (38–84)	38 (22–56)	40 (25–62)	43 (27–69)	48 (31–72)	56 (36–80)
Vegetables	45 (29–66)	63 (43–94)	80 (52–118)	105 (73–730)	744 (117–812)	57 (37–85)	80 (52–118)	99 (69–714)	131 (89–772)	779 (136–824)
Fruit	34 (8–54)	50 (23–80)	61 (34–107)	80 (39–127)	114 (80–161)	54 (23–88)	80 (39–114)	96 (61–127)	114 (80–161)	127 (96–161)
Meat	22 (12–32)	23 (14–35)	25 (14–36)	27 (16–39)	29 (18–43)	26 (14–38)	26 (16–38)	26 (16–39)	27 (16–39)	27 (15–41)
Milk and dairy products	37 (7–146)	73 (7–146)	73 (7–147)	79 (13–147)	97 (17–147)	78 (8–147)	81 (21–151)	106 (31–151)	146 (31–152)	123 (31–152)
Soy	15 (13–32)	30 (15–39)	32 (15–50)	39 (21–629	50 (32–69)	21 (15–32)	32 (15–50)	32 (21–62)	39 (32–62)	62 (39–70)
Selected nutrient intakes[2]										
Vitamin B-6, *mg/d*	0.8 (0.6–1.0)	0.9 (0.7–1.1)	1.0 (0.8–1.2)	1.1 (0.9–1.3)	1.3 (1.1–1.5)	0.8 (0.7–1.0)	0.9 (0.8–1.1)	1.0 (0.9–1.2)	1.1 (1.0–1.3)	1.3 (1.1–1.5)
(n-3) Fatty acids, *mg/d*	1.1 (0.8–1.5)	1.3 (1.0–1.8)	1.5 (1.2–2.0)	1.7 (1.4–2.2)	2.1 (1.7–2.6)	1.2 (0.9–1.6)	1.4 (0.8–1.8)	1.5 (1.2–2.0)	1.7 (1.4–2.2)	2.1 (1.6–2.6)
Calcium, *mg/d*	273 (270–493)	440 (330–551)	492 (370–606)	554 (429–660)	634 (514–747)	415 (297–527)	470 (343–583)	518 (386–624)	566 (437–670)	626 (494–739)
Potassium, *mg/d*	1736 (1394–2096)	2004 (1651–2371)	2229 (1872–2626)	2525 (2154–2911)	3008 (2614–3450)	1879 (1519–2246)	2114 (1763–2482)	2333 (1982–2700)	2590 (2236–2949)	2995 (2603–3391)
Sodium, *mg/d*	1319 (965–1772)	1778 (1312–2318)	2167 (1675–3140)	2498 (2006–2965)	2954 (2475–3485)	1335 (1001–1772)	1675 (1282–2168)	1997 (1535–2474)	2315 (1827–2778)	2731 (2246–3218)
Isoflavones, *mg/d*	12 (7–24)	25 (12–38)	34 (19–42)	39 (28–46)	46 (38–51)	12 (7–19)	19 (12–33)	28 (17–40)	37 (24–44)	44 (34–51)
SFA, *g/d*	8 (6–10)	9 (6–11)	9 (7–12)	10 (8–12)	11 (8–13)	9 (6–11)	9 (7–12)	10 (7–12)	10 (8–12)	11 (8–13)
Monounsaturated fatty acids, *g/d*	8 (6–10)	9 (7–11)	9 (7–12)	10 (8–12)	12 (9–14)	9 (6–11)	9 (7–11)	10 (8–12)	10 (8–12)	11 (9–14)
PUFA, *g/d*	5 (4–6)	6 (5–7)	7 (6–8)	8 (6–9)	9 (8–11)	5 (4–7)	6 (5–7)	7 (5–8)	7 (6–9)	9 (7–10)
Cholesterol, *g/d*	213 (142–316)	240 (161–332)	263 (183–349)	297 (205–367)	339 (236–401)	220 (148–323)	238 (166–336)	261 (183–349)	287 (199–365)	318 (218–390)
Energy, *kJ/d*	7457 (6046–8838)	7000 (5640–8499)	6950 (5585–8503)	7013 (5740–8520)	7281 (6125–8851)	6021 (5007–7365)	5648 (4794–6590)	5748 (4911–6590)	5954 (5120–6757)	6259 (5313–7155)
Keys score,[3] *mmol/L*	0.62 (0.51–0.74)	0.67 (0.56–0.80)	0.69 (0.57–0.82)	0.72 (0.61–0.84)	0.74 (0.62–0.86)	0.74 (0.60–0.88)	0.80 (0.67–0.93)	0.81 (0.69–0.93)	0.82 (0.69–0.93)	0.82 (0.69–0.92)
Serum chemistry of subsample, *n* = 19,869										
Participants at risk, *n*	1403	1383	1378	1317	1286	2964	2807	2571	2434	2326
Total cholesterol, *mmol/L*	4.9 (4.3–5.5)	4.8 (4.3–5.5)	4.9 (4.3–5.5)	4.8 (4.2–5.4)	4.8 (4.3–5.4)	5.2 (4.6–5.8)	5.2 (4.6–5.9)	5.2 (4.6–5.9)	5.2 (4.7–5.8)	5.1 (4.5–5.7)
HDL-cholesterol, *mmol/L*	1.3 (1.1–1.6)	1.3 (1.1–1.6)	1.3 (1.1–1.6)	1.3 (1.1–1.5)	1.3 (1.1–1.6)	1.4 (1.2–1.6)	1.4 (1.2–1.7)	1.4 (1.2–1.6)	1.4 (1.2–1.6)	1.4 (1.2–1.6)
Triglycerides, *mmol/L*	1.3 (0.87–1.9)	1.2 (0.87–1.8)	1.3 (0.87–1.8)	1.2 (0.88–1.7)	1.2 (0.88–1.7)	1.2 (0.83–1.6)	1.1 (0.77–1.5)	1.1 (0.84–1.6)	1.1 (0.77–1.5)	1.1 (0.77–1.5)

[1] Values are median (interquartile range), or percentages.

[2] Food and nutrient intakes were energy-adjusted using the residual method.

[3] Keys score was calculated by this formula: Keys score = 1.35[2 [energy from SFA (% energy)] – [energy from PUFA (% energy)] + 1.52 [cholesterol intake (mg/1000 kcal)]².

TABLE 2 Sex-specific HR and 95% CI for mortality from CVD according to quintiles of TDF intake

	Men						Women					
	Q1 (Low)	Q2	Q3	Q4	Q5 (High)	*P*-trend[1]	Q1 (Low)	Q2	Q3	Q4	Q5 (High)	*P*-trend[1]
n	4623	4624	4624	4624	4624		7122	7122	7122	7122	7122	
Range, *g/d*	<7.8	7.8–9.4	9.5–10.8	10.9–12.6	>12.6		<8.5	8.5–9.9	10.0–11.1	11.2-12.7	>12.7	
Person-years	57,080	57,426	57,863	57,901	58,247		89,055	89,450	90,951	91953	93241	
Total stroke												
Cases, *n*	60	149	119	91	80		71	87	102	128	116	
Age-adjusted HR (95%CI)	1	1.32 (0.94–1.70)	1.37 (0.96–1.77)	1.33 (0.93–1.70)	1.03 (0.76–1.37)	0.642	1	0.97 (0.78–1.21)	1.01 (0.82–1.24)	1.13 (0.92-1.38)	1.19 (0.97-1.45)	0.364
Multivariable HR (95%CI)[2]	1	1.14 (0.74–1.76)	1.12 (0.74–1.69)	1.15 (0.70–1.56)	1.09 (0.75–1.58)	0.555	1	0.78 (0.55–1.12)	1.08 (0.76–1.54)	0.89 (0.61-1.30)	1.05 (0.73-1.51)	0.775
CHD												
Cases, *n*	40	60	50	41	40		38	35	41	47	30	
Age-adjusted HR (95%CI)	1	0.83 (0.62–1.11)	0.70 (0.52–0.93)	0.60 (0.44–0.82)	0.77 (0.58–1.03)	0.013	1	1.04 (0.74–1.47)	0.85 (0.59–1.14)	0.79 (0.54-0.98)	0.79 (0.54-0.96)	0.021
Multivariable HR (95%CI)[2]	1	0.83 (0.62–1.12)	0.69 (0.51–0.93)	0.59 (0.43–0.81)	0.81 (0.61–1.09)	0.022	1	1.03 (0.76–1.48)	0.86 (0.61–1.13)	0.81 (0.52-0.99)	0.80 (0.57-0.97)	0. 014
Other CVD												
Cases, *n*	45	94	75	64	55		52	51	78	86	75	
Age-adjusted HR (95%CI)	1	1.35 (0.93–1.97)	1.05 (0.74–1.51)	1.07 (0.62–1.34)	0.99 (0.68–1.45)	0.464	1	1.13 (0.86–1.49)	0.99 (0.60–1.41)	0.87 (0.59-1.29)	1.11 (0.86-1.44)	0.254
Multivariable HR (95%CI)[2]	1	1.25 (0.87–1.79)	0.92 (0.65–1.32)	1.06 (0.62–1.36)	0.78 (0.54–1.13)	0.313	1	1.18 (0.91–1.54)	0.97 (0.74–1.26)	0.78 (0.55-1.10)	1.06 (0.74-1.51)	0.212
Total CVD												
Cases, *n*	145	303	244	196	175		161	153	221	261	221	
Age-adjusted HR(95%CI)	1	1.02 (0.88–1.17)	0.91 (0.79–1.05)	0.84 (0.52–1.08)	0.84 (0.66–1.02)	0.043	1	1.17 (0.89–1.39)	1.10 (0.86–1.26)	0.84 (0.68-1.04)	0.81 (0.57-0.98)	0.061
Multivariable HR (95%CI)[2]	1	1.06 (0.92–1.22)	0.92 (0.80–1.06)	0.86 (0.55–1.15)	0.83 (0.63–1.09)	0.054	1	1.21 (0.94–1.44)	1.06 (0.82–1.19)	0.85 (0.69-0.99)	0.82 (0.57-0.97)	0.044

[1] Based on tests for trend across quintiles of fiber intake by assigning the median value of each quintile.

[2] Cox proportional hazard model adjusted for age, BMI, history of hypertension, history of diabetes, alcohol consumption, smoking, education level, hours of exercise, hours of walking, perceived mental stress, sleep fish, SFA, (n-3) fatty acids, sodium, folate, and vitamin E.

TABLE 3 Sex-specific HR and 95% CI for mortality from CVD according to quintiles of IDF and SDF intakes

	Men						Women					
	Q1 (Low)	Q2	Q3	Q4	Q5 (High)	*P*-trend[1]	Q1 (Low)	Q2	Q3	Q4	Q5 (High)	*P*-trend[1]
n	4623	4624	4624	4624	4624		7122	7122	7122	7122	7122	
IDF												
Range, *g/d*	<5.9	5.9–6.9	7.0–7.9	8.0–9.2	>9.2		<6.2	6.2–7.1	7.2–8.0	8.1-9.1	>9.1	
Person-years	56,963	57,598	57,534	57,720	58,702		89,073	89,584	90,918	91854	93220	
Total stroke												
Cases, *n*	61	77	108	144	109		64	137	100	111	72	
Age-adjusted HR (95%CI)	1	0.97 (0.70–1.36)	1.12 (0.82–1.54)	1.03 (0.76–1.39)	0.98 (0.71–1.34)	0.945	1	1.10 (0.82–1.49)	1.20 (0.87–1.64)	1.13 (0.83-1.54)	0.93 (0.67-1.31)	0.344
Multivariable HR (95%CI)[2]	1	1.01 (0.70–1.46)	1.16 (0.79–1.70)	0.98 (0.64–1.52)	0.96 (0.64–1.45)	0.715	1	1.03 (0.70–1.51)	1.18 (0.83–1.69)	1.06 (0.73-1.53)	0.90 (0.63-1.28)	0.128
CHD												
Cases, *n*	44	38	40	61	48		39	44	35	38	35	
Age-adjusted HR (95%CI)	1	0.69 (0.45–1.07)	0.62 (0.40–0.96)	0.68 (0.46–1.01)	0.65 (0.43–0.98)	0.032	1	0.72 (0.46–1.14)	0.66 (0.42–1.05)	0.60 (0.38-0.94)	0.53 (0.34-0.82)	0.003
Multivariable HR (95%CI)[2]	1	0.63 (0.39–1.02)	0.52 (0.30–0.87)	0.46 (0.26–0.84)	0.48 (0.27–0.84)	<0.001	1	0.63 (0.38–1.04)	0.61 (0.36–1.03)	0.56 (0.33-0.98)	0.49 (0.27-0.86)	0.004
Other CVD												
Cases, *n*	48	49	72	92	72		49	88	73	81	51	
Age-adjusted HR (95%CI)	1	1.43 (0.95–2.14)	1.01 (0.70–1.46)	1.13 (0.80–1.61)	1.24 (0.85–1.79)	0.715	1	0.86 (0.60–1.22)	0.94 (0.65–1.36)	1.01 (0.71-1.44)	1.06 (0.71-1.57)	0.325
Multivariable HR (95%CI)[2]	1	1.24 (0.85–2.06)	1.01 (0.68–1.21)	1.06 (0.69–1.49)	1.15 (0.78–1.62)	0.798	1	0.83 (0.48–1.45)	1.09 (0.67–1.77)	1.20 (0.73-1.99)	0.83 (0.51-1.33)	0.698
Total CVD												
Cases, *n*	153	164	220	297	229		152	269	208	230	158	
Age-adjusted HR (95%CI)	1	0.88 (0.72–1.07)	0.99 (0.84–1.17)	0.91 (0.78–1.08)	0.85 (0.68–1.03)	0.061	1	0.84 (0.67–1.04)	0.93 (0.76–1.15)	0.87 (0.71-1.06)	0.84 (0.68-1.03)	0.301
Multivariable HR (95%CI)[2]	1	0.88 (0.68–1.04)	0.97 (0.79–1.08)	0.89 (0.72–1.03)	0.82 (0.65–0.98)	0.042	1	0.78 (0.61–1.00)	0.82 (0.64–1.06)	0.68 (0.51-0.91)	0.69 (0.53-0.91)	0.017
SDF												
Range, *g/d*	<1.3	1.3–1.6	1.7–1.9	2.0–2.3	>2.3		<1.5	1.5–1.8	1.9–2.1	2.2-2.4	>2.4	
Person-years	57,151	57,436	57,798	57,903	58,230		89,551	89,205	90,778	91613	93503	
Total stroke												
Cases, *n*	65	146	107	90	91		78	72	125	107	102	
Age-adjusted HR (95%CI)	1	1.04 (0.77–1.40)	0.95 (0.69–1.29)	1.11 (0.81–1.53)	0.92 (0.67–1.27)	0.991	1	0.81 (0.59–1.12)	0.91 (0.69–1.21)	1.00 (0.75-1.34)	1.07 (0.80-1.44)	0.901
Multivariable HR (95%CI)[2]	1	0.98 (0.66–1.47)	0.91 (0.61–1.34)	1.12 (0.79–1.59)	0.90 (0.61–1.31)	0.790	1	0.80 (0.57–1.12)	0.86 (0.61–1.24)	0.95 (0.67-1.34)	1.02 (0.73-1.42)	0.643
CHD												
Cases, *n*	38	59	46	43	45		39	39	41	38	34	
Age-adjusted HR (95%CI)	1	0.81 (0.53–1.22)	0.83 (0.54–1.19)	0.74 (0.61–1.10)	0.76 (0.49–1.07)	0.092	1	0.98 (0.55–1.14)	0.56 (0.36–0.87)	0.74 (0.44-1.04)	0.69 (0.44-0.97)	0.005
Multivariable HR (95%CI)[2]	1	0.80 (0.44–1.16)	0.81 (0.48–1.17)	0.72 (0.58–1.02)	0.71 (0.41–0.97)	0.043	1	0.86 (0.54–1.18)	0.60 (0.34–1.04)	0.88 (0.54-1.07)	0.72 (0.43-0.99)	0.035
Other CVD												
Cases, *n*	46	96	71	59	61		56	56	88	65	77	
Age-adjusted HR (95%CI)	1	1.43 (1.00–2.04)	1.41 (0.97–2.06)	1.11 (0.87–1.88)	1.12 (0.88–1.69)	0.765	1	0.79 (0.54–1.16)	0.74 (0.53–1.04)	1.18 (0.82-1.69)	0.84 (0.60-1.19)	0.312
Multivariable HR (95%CI)[2]	1	1.09 (0.86–1.75)	1.24 (0.79–1.87)	1.04 (0.88–1.76)	1.08 (0.75–1.64)	0.573	1	0.74 (0.48–1.14)	0.77 (0.46–1.28)	1.32 (0.81-2.15)	0.96 (0.61-1.50)	0.613
Total CVD												
Cases, *n*	149	301	224	192	197		173	167	254	210	213	
Age-adjusted HR (95%CI)	1	1.23 (0.79–1.88)	1.04 (0.72–1.39)	0.75 (0.54–0.97)	0.82 (0.62–1.08)	0.052	1	0.81 (0.67–0.98)	0.84 (0.68–1.04)	0.77 (0.61-0.97)	0.80 (0.56-0.99)	0.021
Multivariable HR (95%CI)[2]	1	1.11 (0.64–1.33)	0.89 (0.69–1.13)	0.74 (0.52–0.98)	0.81 (0.53–1.04)	0.042	1	0.86 (0.68–1.07)	0.85 (0.67–1.09)	0.79 (0.65-0.98)	0.83 (0.53-1.02)	0.043

[1] Based on tests for trend across quintiles of fiber intake by assigning the median value of each quintile.

[2] Cox proportional hazard model adjusted for age, BMI, history of hypertension, history of diabetes, alcohol consumption, smoking, education level, hours of exercise, hours of walking, perceived mental stress, sleep ho fish, SFA, (n-3) fatty acids, sodium, folate, and vitamin E.

TABLE 4 Sex-specific HR and 95% CI for mortality from CHD according to quintiles of cereal, fruit, and vegetable fiber intakes

	Men						Women					
	Q1 (Low)	Q2	Q3	Q4	Q5 (High)	*P*-trend[1]	Q1 (Low)	Q2	Q3	Q4	Q5 (High)	*P*-trend[1]
n	4623	4624	4624	4624	4624		7122	7122	7122	7122	7122	
Cereal fiber												
Range, *g/d*	<1.4	1.4–1.6	1.7–1.8	1.9–2.1	>2.1		<1.1	1.1–1.3	1.4–1.5	1.6–1.7	>1.7	
Person-years	57,289	57,650	57,640	57,651	58,288		90,356	90,793	91,764	90516	91224	
Cases, *n*	45	50	51	40	45		49	33	28	49	32	
Age-adjusted HR (95%CI)	1	0.92 (0.73–1.16)	0.96 (0.71–1.25)	0.81 (0.66–1.03)	0.88 (0.71–1.05)	0.125	1	0.79 (0.52–0.96)	0.74 (0.56–0.95)	1.03 (0.83–1.54)	0.76 (0.57–0.98)	0.044
Multivariable HR (95%CI)[2]	1	0.90 (0.70–1.16)	0.92 (0.69–1.12)	0.77 (0.64–0.98)	0.86 (0.64–0.99)	0.042	1	0.80 (0.53–0.97)	0.73 (0.53–0.97)	1.06 (0.73–1.53)	0.77 (0.59–0.98)	0.031
Multivariable HR (95%CI)[3]	1	0.89 (0.68–1.15)	0.90 (0.68–1.16)	0.74 (0.61–0.99)	0.89 (0.65–1.01)	0.060	1	0.80 (0.53–0.98)	0.74 (0.50–0.89)	1.06 (0.74–1.56)	0.76 (0.59–0.97)	0.044
Fruit fiber												
Range, *g/d*	<0.4	0.4–0.7	0.8–1.0	1.1–1.7	>1.7		<0.7	0.7–1.1	1.2–1.8	1.9–2.2	>2.2	
Person-years	57,199	57,641	57,971	57,891	57,816		90,999	90,382	90,751	90079	92438	
Cases, *n*	62	53	43	36	37		55	39	36	39	22	
Age-adjusted HR (95%CI)	1	0.79 (0.46–1.01)	0.69 (0.54–0.98)	0.54 (0.36–0.82)	0.54 (0.35–0.86)	0.004	1	0.69 (0.45–1.05)	0.67 (0.45–1.01	0.66 (0.34–0.98)	0.43 (0.26–0.70)	0.003
Multivariable HR (95%CI)[2]	1	0.80 (0.45–1.03)	0.71 (0.53–0.99)	0.54 (0.37–0.86)	0.56 (0.35–0.90)	0.007	1	0.71 (0.43–1.08)	0.70 (0.43–1.02	0.65 (0.31–0.98)	0.40 (0.28–0.78)	0.005
Multivariable HR (95%CI)[3]	1	0.82 (0.45–1.09)	0.75 (0.52–1.02)	0.55 (0.34–0.92)	0.55 (0.32–0.96)	0.032	1	0.73 (0.42–1.10)	0.69 (0.42–1.04)	0.63 (0.33–0.99)	0.42 (0.33–0.81)	0.014
Vegetable fiber												
Range, *g/d*	<2.8	2.8–3.6	3.7–4.3	4.4–5.5	>4.5		<3.1	3.1–3.9	4.0–4.6	4.7–5.6	>5.6	
Person-years	57,636	58,016	57,735	57,989	57,140		89,688	90,396	90,874	91592	92099	
Cases, *n*	40	42	40	48	61		36	34	36	43	42	
Age-adjusted HR (95%CI)	1	1.04 (0.66–1.62)	1.15 (0.75–1.77)	0.77 (0.49–1.21)	0.90 (0.58–1.38)	0.328	1	0.76 (0.46–1.26)	0.92 (0.58–1.47)	0.64 (0.40–1.05)	0.79 (0.51–1.24)	0.460
Multivariable HR (95%CI)[2]	1	1.06 (0.66–1.71)	1.16 (0.72–1.89)	0.76 (0.46–1.28)	0.92 (0.56–1.52)	0.417	1	0.79 (0.47–1.34)	0.96 (0.58–1.60)	0.73 (0.43–1.24)	0.91 (0.55–1.49)	0.983
Multivariable HR (95%CI)[3]	1	1.03 (0.64–1.67)	1.14 (0.70–1.86)	0.75 (0.44–1.26)	0.90 (0.54–1.51)	0.666	1	0.78 (0.46–1.32)	0.93 (0.56–1.55)	0.73 (0.43–1.25)	0.97 (0.58–1.62)	0.917

[1] Based on tests for trend across quintiles of fiber intake by assigning the median value of each quintile.
[2] Cox proportional hazard model adjusted for age, BMI, history of hypertension, history of diabetes, alcohol consumption, smoking, education level, hours of exercise, hours of walking, perceived mental stress, sleep hour fish, SFA, (n-3) fatty acids, sodium, folate, and vitamin E.
[3] Adjusted further for other types of dietary fiber (cereal, fruit, and vegetable fibers).